Computers and Chemical Engineering 133 (2020) 106651

Contents lists available at ScienceDirect

Computers and Chemical Engineering

journal homepage: www.elsevier.com/locate/compchemeng

Modeling, simulation and optimization of combined fractional-ordinary dynamic systems

Vicente Rico-Ramirez[a], Julio C. Barrera-Martinez[a], Edgar O. Castrejon-Gonzalez[a], Edna S. Lopez-Saucedo[a], Urmila M. Diwekar[b,*]

[a] Tecnologico Nacional de Mexico en Celaya, Departamento de Ingenieria Quimica, Av., Tecnologico y Garcia Cubas S/N, Celaya, Guanajuato 38010, Mexico
[b] Vishwamitra Research Institute, 368 56th Street, Clarendon Hills, IL 60514, USA

ARTICLE INFO

Article history:
Received 12 August 2019
Revised 28 October 2019
Accepted 17 November 2019
Available online 18 November 2019

Keywords:
Fractional calculus
Compartmental modeling
Fractional-ordinary model
Fractional optimal control problem

ABSTRACT

This work proposes an approach to the modeling and optimization of systems involving a coupled set of fractional and ordinary differential equations. We first present a generalized version of the predictor-corrector integration method, which can integrate simultaneously both fractional and ordinary differential equations. Further, we describe an analytical/numerical dynamic optimization strategy that combines the generalized optimality conditions for a fractional-ordinary system derived in this work, the generalized integration technique and the gradient method. The approach is illustrated through a compartmental model in pharmacokinetics as well as a fractional model for a thermal hydrolysis. In both cases, after we apply a formal fractionalization strategy, we propose a reformulation of the models to obtain fractional-ordinary dynamic systems. The systems obtained are further posed within an optimization framework and solved through our approach as fractional-ordinary optimal control problems. Our results show the theoretical and numerical consistency of our approach.

1. Introduction: fractional calculus and operators

Various engineering applications have recently demonstrated the modeling capabilities of fractional calculus; such concept, which introduces derivatives and integrals of non-integer order, has been used to represent the behavior of complex phenomena in several areas, including rheology (viscoelastic fluids), heat diffusion, interfacial mass transfer, process control, electrochemistry, classical mechanics, chaos, fractals, immunotherapy, epidemiology, sensor development and many other fields (Lopes et al., 2019; Sarafnia et al., 2018; Sápi et al., 2017; Sopasakis and Sarimveis, 2017; Flores-Tlacuahuac and Biegler, 2014; Diethelm, 2013; Ding et al., 2012; Almeida and Torres, 2011; Kovács et al, 2011; Magin, 2010;Tenreiro-Machado et al., 2010). Compartmental models for drug absorption, distribution and elimination within the body (pharmacokinetics) have also been formulated with the aid of fractional calculus (Pereira, 2010). Various contributions involve applications to the administration of particular drugs; for instance, amiodarone (Dokoumetzidis et al., 2010b), diclofenac and bumetanide (Popovic et al., 2010), propofol (Copot et al., 2013) and doxorubicin (Ionescu et al., 2016). Further, recent contributions describe the significance of fractional calculus for modeling biological phenomena in a more general sense, and show how fractional kinetics are natural solutions to the diffusion problems in biological tissues (Ionescu et al., 2017; Ionescu and Kelly, 2017; Copot et al, 2017a; Copot et al, 2017b; Ionescu et al., 2015; Ionescu et al, 2013; Petráš and Magin, 2011;); interesting phenomena, such as drug tissue trapping and tissue heterogeneity, have been addressed in those works. Finally, the work by Sun et al. (2018) provides an excellent review of real-world applications of fractional calculus in various engineering fields, which can motivate further methods and model developments on this topic.

1.1. Fractional operators

The modeling capabilities of fractional calculus are mostly due to the non-local property of fractional operators, which can be used to represent the behavior of state variables showing memory effects. The literature reports several definitions for the fractional derivative, including the expressions derived by Riemann–Liouville, Caputo, Riesz, Riesz–Caputo, Weyl, Grunwald–Letnikov, Hadamard and Chen (Sales Teodoro et al, 2019); however, the definitions by Riemann–Liouville and Caputo are the most widely used. The left Caputo definition for the fractional derivative of function $f(x)$ is given by Eq. (1), where D is used to represent the fractional op-

* Corresponding author.
E-mail address: urmila@vri-custom.org (U.M. Diwekar).

https://doi.org/10.1016/j.compchemeng.2019.106651
0098-1354/

erator, C stands for Caputo, x is the independent variable, α is a positive real number (order of derivative), n is an integer number such that $n\text{-}1<\alpha<n$ and Γ is the Gamma function:

$$ {}_a^C D_x^\alpha f(x) = \frac{1}{\Gamma(n-\alpha)} \int_a^x (x-t)^{n-\alpha-1} f^{(n)}(t)dt \tag{1} $$

Observe that memory effects are introduced through a convolution integral (the derivative at a given point depends on the whole dynamic behavior of the variable) included in the various definitions. The Caputo differential operator is linear, so that Eq. (2) applies for any arbitrary constant α and for arbitrary functions $f(x)$ and $g(x)$, as long as their integrals exist; further, the operator satisfies the commutative property given by Eq. (3) for any arbitrary constants α and β (Diethelm et al., 2005):

$$ {}_a^C D_x^\alpha (a_1 f(x) + a_2 g(x)) = a_1 {}_a^C D_x^\alpha f(x) + a_2 {}_a^C D_x^\alpha g(x) \tag{2} $$

$$ {}_0^C D_x^\alpha \left({}_0^C D_x^\beta f(x) \right) = {}_0^C D_x^\beta \left({}_0^C D_x^\alpha f(x) \right) = {}_0^C D_x^{\alpha+\beta} f(x) \tag{3} $$

Additionally, the Caputo fractional derivative of a constant, c, is zero:

$$ {}_a^C D_x^\alpha (c) = 0 \tag{4} $$

Similarly, the left Riemann–Liouville fractional integral definition is given by Eq. (5):

$$ {}_a I_x^\alpha f(x) = \frac{1}{\Gamma(\alpha)} \int_a^x (x-t)^{\alpha-1} f(t)dt \tag{5} $$

I indicates the fractional integral operator; notice that the superscript C is not included, since this expression is a Riemann-Liouville definition. Finally, as expected, fractional integration and fractional derivative operators are inverse operators (Almeida and Torres, 2011):

$$ {}_a D_x^\alpha \, {}_a I_x^\alpha f(x) = f(x) \tag{6} $$

1.2. Numerical algorithms for the simulation and optimization of fractional models

Several numerical/theoretical tools have been developed for the simulation and optimization of dynamic systems of fractional differential equations. The most relevant works to our approach are summarized in this section.

1.2.1. Numerical integration of sets of fractional differential equations

Literature reports several recent efforts to integrate fractional differential equations by numerical methods; among them, there are some fundamental approaches for particular problems (Mendes et al, 2019; Moghaddam et al, 2019). As a most general case, Garrapa (2018) presents an excellent review of some of the most efficient existing multi-step methods for integrating fractional differential equations (FDE), and provides Matlab functions to perform numerical simulations through some of such techniques. The author describes both Product Integration (PI) methods and Fractional Linear Multi-step Methods (FLMMs). The predictor-corrector method of Diethelm et al. (2002, 2004, 2005) and Diethelm (2010) is among the best known PI techniques; on the other hand, FLMMs are illustrated through various developments such as the method of Lubich (1986) and the Grunwald–Letnikov scheme. Besides the numerical strategies, Garrapa (2018) also discusses the three types of problems involving fractional order operators (Fractional Differential Equations (FDE), Multi-order systems (MOS) and Linear Multi-Term FDEs) which can be addressed through multi-step methods.

The algorithm provided by Diethelm et al. (2002, 2004, 2005) is one of the most widely used methods for integrating FDE and has been selected as one of the basis of this work. This method is an extension of the predictor-corrector method of the Adams-Bashforth-Moulton technique, so that it could be applied to the fractional case. The algorithm can be applied to the initial value problem:

$$ \begin{aligned} {}_0^C D_t^\alpha y(t) &= f(t, y(t)) \\ y^{(k)}(0) &= y_0^k, \; k = 0, 1, 2, \ldots, m-1 \end{aligned} \tag{7} $$

where the fractional order is $\alpha > 0$ and $m = [\alpha]$; notice that only fractional differential equations are considered; y is the dependent variable and t is the independent variable. k is related to the order of the fractional derivative and to the number of initial conditions for each differential equation. By applying the formula of the rectangular quadrature rule, a predictor step is calculated by Eq. (8):

$$ y^P(t_{n+1}) = \sum_{k=0}^{\alpha-1} y_0^{(k)} \frac{t_{n+1}^k}{k!} + \frac{1}{\Gamma(\alpha)} \sum_{j=0}^{n} b_{j,n+1} f\left(t_j, y\left(t_j\right)\right) \tag{8} $$

where

$$ b_{j,n+1} = \frac{h^\alpha}{\alpha} \left((n+1-j)^\alpha - (n-j)^\alpha \right) \tag{9} $$

and h is the integration time step. Then, by using a trapezoidal quadrature rule, the corrector step is defined as follows:

$$ \begin{aligned} y(t_{n+1}) = &\sum_{k=0}^{\alpha-1} y_0^{(k)} \frac{t_{n+1}^k}{k!} + \frac{h^\alpha}{\Gamma(\alpha+2)} f\left(t_{n+1}, y^P(t_{n+1})\right) \\ &+ \frac{h^\alpha}{\Gamma(\alpha+2)} \sum_{j=0}^{n} a_{j,n+1} f\left(t_j, y\left(t_j\right)\right) \end{aligned} \tag{10} $$

where

$$ a_{j,n+1} = \begin{cases} n^{\alpha+1} - (n-\alpha)(n+1)^\alpha, & \text{if } j = 0 \\ (n-j+2)^{\alpha+1} + (n-j)^{\alpha+1} - 2(n-j+1)^{\alpha+1}, & \text{if } 1 \le j \le n \\ 1, & \text{if } j = n+1 \end{cases} \tag{11} $$

1.2.2. Optimizing dynamic systems of fractional differential equations: solution of fractional optimal control problems

When a set of fractional differential equations is posed within an optimization framework, the result is a fractional optimal control problem. Various numerical as well as theoretical tools have been developed for optimizing fractional systems (Wei et al., 2017). The classical works by Agrawal (2002; 2004; 2007; 2008; 2010) present the derivations for the optimality conditions (Euler-Lagrange Equations) for such problems, including the variations resulting from the use of different definitions of fractional derivatives. Similar optimality conditions have also been derived by Guo (2013), Herzallah and Baleanu (2009), Baleanu and Trujillo (2010), Jelicic and Petrovacki (2009) and Jahanshahi and Torres (2017). Further, Atanackovic et al. (2017) considered the case of complex fractional order derivatives, whereas Caputo and Caputo–Fabrizio fractional derivatives have also been included in the problem definition (Almeida, 2017; Nuno and Bastos; 2018). The Euler–Lagrange equations for a fractional optimal control problem consist of a two-point boundary value problem involving fractional differential equations. Such boundary value problem has to be solved in order to determine the optimal profiles for the control and state variables. Collocation techniques (Rabiei and Parand, 2019) as well as a direct solution approach based on the Hamilton-Jacobi-Bellman (Rackhshan et al., 2018) have been reported as suitable solution approaches. Among the applications of such fractional optimality conditions, the work by Ding et al. (2012) proposes a formulation to represent the interaction between the immune system

and HIV, and Toledo-Hernandez et al. (2014b) propose a numerical strategy for the optimization of fractional biological reactive systems.

2. Modeling and optimization of fractional-ordinary models

We believe that most of the complex dynamic models that present memory effects in some of their components will also present a conventional ordinary behavior in any other of their parts. Therefore, general dynamic systems will most certainly include a set of differential equations that involves both fractional as well as ordinary differential equations. Therefore, numerical and theoretical tools for those combined problems are required. Our work then intends to present a generalized framework for the simulation and optimization of dynamic systems including both ordinary and fractional differential equations. When facing those problems, most of the existing literature proposes a solution approach based on a numerical inverse Laplace transform algorithm, which can be applied for linear systems. As an alternative, this paper presents an approach that does not require such transformation and obtains the solution in the time domain.

2.1. Our approach

The numerical techniques for fractional differentiation and integrations reduce to the ordinary case when the order used is integer. Fractional integration techniques can then be used for integer orders. As a consequence, fractional integration could be used as a general case and the same technique could therefore be applied for the integration of both integer and fractional differential equations. The problem is, however, that the use of a fractional technique for the integration of an ordinary equation is not practical; the computational effort rapidly increases unnecessarily (a local ordinary derivative is estimated through a convolution integral of the whole dynamic behavior of the variable).

Therefore, as a first contribution, we present a generalized version of the predictor-corrector integration method, which can integrate simultaneously both fractional and ordinary differential equation in an efficient manner. Such fractional-ordinary integration technique is used as a basic tool in the other contributions of this work. So, it can then be used along to non-linear correlation techniques for the formulation of fractional-ordinary models in which some of the state variables present memory effects. Also, it can be used for the simulation of those fractional-ordinary models. Nevertheless, we must emphasize that the contribution of this method lies only on the decomposition of the equations and on the numerical implementation of the strategy; the conceptual analysis of this technique and other multi-step methods have already been reported in the literature (Garrapa, 2018).

Further, there are two other main contributions in this work:

(1) In the context of fractional modeling, a common approach used in compartmental modeling starts with an ordinary model. Once memory effects are identified, a formal fractionalization strategy is applied to the ordinary model so that mass balances are preserved. The strategy results in a system of differential equations involving both ordinary and fractional operators in each equation (linear multi-term FDEs). To simulate or optimize such system, an inverse Laplace transformation technique can be applied for linear systems (Dokumetzidis et al., 2010b); similarly, a numerical approximation for the fractional operator can also be given in terms of the Oustaloup Recursive Approximation (ORA) in the frequency domain (Tricaud and Chen, 2010) and through the use of artificial neural networks (Pakdaman et al., 2017). In this work we propose an alternative approach that uses no transformation.

After the fractionalization approach (equations have both fractional and ordinary differential operators), we introduce artificial variables and apply the commutative property for successive fractional derivation so that the multi-linear FDE system can be converted into a set of fractional-ordinary differential equation (SFODE; each equation is either fractional or ordinary). Then, the model can be addressed by our generalized approach for either simulation (generalized numerical integration) or optimization.

(2) As the main contribution of the work, a theoretical/numerical strategy for approaching fractional-ordinary optimal control problems (FOOCP) has also been developed. Such strategy involves the use of a generalized version of the Euler–Lagrange optimality conditions for a fractional-ordinary system. Such conditions are derived and then resolved by a gradient based method to obtain the optimal profiles for the state and control variables.

Two case studies are used in this work. The first one is a compartmental model for drug absorption and distribution within the body. A second example considers a model for mezcal (an alcoholic beverage made from agave) production (a thermal hydrolysis). Both examples have already been simulated and optimized in the literature by different numerical approaches, so that we can perform a direct comparison to assess the performance of our approach.

3. Development of theoretical and numerical tools for the simulation and optimization of fractional-ordinary models

This section describes the main numerical/theoretical contributions of this paper. The work presents a theoretical/numerical approach to simulate and optimize dynamical systems involving both fractional and ordinary differential equations. This is a general topic that can be applied to most of the engineering areas, including chemical engineering. For instance, literature reports show the application of fractional calculus to rheology (West et al., 2003; Yang and Zhu, 2011), process control (Aguila-Camacho and Duarte-Mermoud, 2017; Sopasakis and Sarimveis, 2017; Sarafnia et al., 2018) and diffusive heat and mass transfer processes (Zecova and Terpak, 2015; Magin, 2004). Nevertheless, there are very few reports about fractional calculus in the classical chemical engineering literature (Flores-Tlacuahuac and Biegler, 2014; Toledo-Hernandez et al., 2014a). The development of the tools provided here is expected to contribute in increasing the attention of the chemical engineering community about this research area.

Notice that the tools implemented in this work were derived directly from the algorithms developed independently for fractional and ordinary models. In both of the algorithms, numerical integration and dynamic optimization, the tools and the derivations provided in the literature for each case were combined into a single general method/technique. The details are as follows.

Many other theoretical issues are significant for the simulation and optimization of fractional dynamic problems, such as the stability of the system. Those issues, however, are out of the scope of this work. For an interesting analysis and the description of theoretical developments on the issue of stability, see the work of Li et al. (2009); the authors describe the Lyapunov direct method for fractional systems and the Mittag–Leffler stability theory.

3.1. Numerical integration of a set of fractional-ordinary differential equations (SFODE)

The generalized version of the numerical integration algorithm, at each time step, includes the estimation of the time history for those state variables presenting memory effects as well as the conventional estimation for those state variables presenting an ordinary behavior. To simplify the presentation of the algorithm, let $\boldsymbol{x}$ be the vector of state variables of a fractional-ordinary dynamical system. Such vector is partitioned into two sub-vectors: $\boldsymbol{x}_1$ is the vector of variables having an ordinary behavior and $\boldsymbol{x}_2$ is the vector of variables presenting memory effects (fractional behavior). $\boldsymbol{x}_1$

is an $n_o$dimensional vector and $\boldsymbol{x}_2$ is an n_f dimensional vector. The fractional-ordinary initial value problem is then given by:

$$\begin{aligned} &\frac{dx_{1_k}}{dt} = G_k(\boldsymbol{x}_1, \boldsymbol{x}_2, t) \quad k = 1, 2, \ldots, n_o \\ &\boldsymbol{x}_1(0) = \boldsymbol{x}_{10} \end{aligned} \tag{12}$$

$$\begin{aligned} &{}_0^C D_t^{\alpha_l} x_{2_l} = F_l(\boldsymbol{x}_1, \boldsymbol{x}_2, t) \quad l = 1, 2, \ldots, n_f \\ &\boldsymbol{x}_2(0) = \boldsymbol{x}_{20} \end{aligned} \tag{13}$$

where the indexes are used to indicate the kth ordinary state variable and the lth fractional state variable with a derivative of order α_l. In Eq. (13), we are assuming that $\alpha_l \in [0, 1]$. $\boldsymbol{G}$ and $\boldsymbol{F}$ represent functions of both the state variables and time. As in the fractional and ordinary cases, for the $n+1$-th point in time (where $n=0$ is the initial condition), the Fractional-Ordinary Predictor–Corrector (FOPC) method involves a predictor step:

$$x_{1_k}{}^P(t_{n+1}) = x_{1_k}(t_n) + hG_k(t_n, \boldsymbol{x}_1(t_n), \boldsymbol{x}_2(t_n)) \quad k = 1, 2, \ldots, n_o \tag{14}$$

$$\begin{aligned} x_{2_l}{}^P(t_{n+1}) \quad = \quad & x_{2_{l_0}} + \frac{1}{\Gamma(\alpha_l)} \sum_{j=0}^{n} b_{j,n+1,l}\, F_l\left(t_j, \boldsymbol{x}_1\left(t_j\right), \boldsymbol{x}_2\left(t_j\right)\right) \\ & l = 1, 2, \ldots, n_f \end{aligned} \tag{15}$$

where $b_{j,n+1,l}$ is given by Eq. (9) for the lth fractional state variable, and a corrector step:

$$\begin{aligned} x_{1_k}(t_{n+1}) = x_{1_k}(t_n) + \frac{h}{2}[&G_k(t_n, \boldsymbol{x}_1(t_n), \boldsymbol{x}_2(t_n)) \\ &+ G_k\left(t_{n+1}, \boldsymbol{x}_1{}^P(t_{n+1}), \boldsymbol{x}_2{}^P(t_{n+1})\right)\Big] \end{aligned} \tag{16}$$

$$\begin{aligned} x_{2_l}(t_{n+1}) \quad = \quad & x_{2_{l_0}} + \frac{h^{\alpha_l}}{\Gamma(\alpha_l + 2)} F_l\left(t_{n+1}, \boldsymbol{x}_1{}^P(t_{n+1}), \boldsymbol{x}_2{}^P(t_{n+1})\right) \\ & + \frac{h^{\alpha_l}}{\Gamma(\alpha_l + 2)} \sum_{j=0}^{n} a_{j,n+1,l}\, F_l\left(t_j, \boldsymbol{x}_1\left(t_j\right), \boldsymbol{x}_2\left(t_j\right)\right) \end{aligned} \tag{17}$$

where $a_{j,n+1,l}$ is given by Eq. (11) for the lth fractional state variable. Eqs. (14) and (16) are simple expressions for ordinary integration and could be replaced by more accurate approaches, as those provided by the Runge-Kutta method. This algorithm has been implemented as a user defined function within the Matlab® environment.

3.2. Euler Lagrange equations (optimality conditions) for a fractional-ordinary optimal control problem (FOOCP)

In general, there are two main approaches to address optimal control problems: direct and indirect methods. In direct transcription methods, both the control and the state variables are discretized and then NLP techniques are used to optimize the system (Andrés-Martínez et al., 2019). On the other hand, indirect methods focus on deriving the optimality conditions of the problem, and additional numerical techniques are then required to solve the resulting two-point boundary value problem. Srinivasan et al. (2003) and Andrés-Martínez et al. (2019) provide a comparison between the methods for the ordinary case.

This paper studies the indirect method, based on the derivation of the optimality conditions. The derivation of the Euler-Lagrange equations for the fractional-ordinary case follows the same general procedure and uses the same concepts as those applied independently to the fractional case (Agrawal, 2010) and to the well known ordinary case. We present here only the main steps of our derivations for the combined problem. Three different forms of the objective function are considered in an FOOCP: Bolza, Lagrange and Mayer forms (Stengel, 1994). In the following derivation, an objective function of Bolza form is assumed, since it is the most general case:

$$J(u) = \varphi\left(\boldsymbol{x}_1\left(t_f\right), \boldsymbol{x}_2\left(t_f\right), t_f\right) + \int_0^{tf} L(\boldsymbol{x}_1(t), \boldsymbol{x}_2(t), u(t), t)dt \tag{18}$$

As before, $\boldsymbol{x}_1$ represents the vector of variables that show first order dynamics; $\boldsymbol{x}_2$ is used to indicate those state variables described by fractional order dynamics($0 < \alpha < 1$). $J(u)$ represents the objective function, which consists of two parts; the first part (φ) is a scalar, continuously differentiable, function dependent on the state variables at the final time, t_f. The second part is an integral term of the function (L) that depends on the state and control variables, $u(t)$, along the whole time interval; L is also assumed to be continuously differentiable. Finally, $J(u)$ should be defined so that the optimal control problem is bounded and feasible.

The constraints of the FOOCP include bounds to the control variables, $u_{min} \le u(t) \le u_{max}$, the set of first order differential equations:

$$\begin{aligned} \frac{d\boldsymbol{x}_1}{dt} \quad &= \quad \boldsymbol{G}(\boldsymbol{x}_1, \boldsymbol{x}_2, u, t) \\ \boldsymbol{x}_1(0) \quad &= \quad \boldsymbol{x}_{1,0} \end{aligned} \tag{19}$$

and the set of fractional order differential equations:

$$\begin{aligned} {}_0^C D_t^{\alpha} \boldsymbol{x}_2 \quad &= \quad \boldsymbol{F}(\boldsymbol{x}_1, \boldsymbol{x}_2, u, t) \\ \boldsymbol{x}_2(0) \quad &= \quad \boldsymbol{x}_{2,0} \end{aligned} \tag{20}$$

The initial conditions for both of the sets of state variables are known. $\boldsymbol{G}$ and $\boldsymbol{F}$ are functions of time as well as the state variables. For simplicity in the representation and in the derivations, it is assumed here that all of the fractional differential equations have the same fractional order, α. From the numerical point of view, the fractional orders can be different for each of the fractional equations, since our approach is not limited in that sense. However, we should notice that, at the current state, our approach does not include any particular consideration to address noncommensurate systems. Therefore, special care must be taken when the state vectors contain elements with different physical units.

For a fractional-only optimal control problem, Agrawal (2004, 2008) provided the optimality conditions when the fractional derivatives assume either the Riemann-Liouville or the Caputo definitions and when the objective function is either in Lagrangian or linear Mayer form (Stengel, 1994).

In this paper, our following derivation integrates the works of Agrawal (2004, 2008) for fractional equations and the conventional variational calculus approach for an ordinary optimal control problem.

As the first step of the derivation, Eq. (18) is reformulated by including the Lagrange multipliers, $\boldsymbol{\lambda}$:

$$\begin{aligned} \bar{J}(u) \quad = \quad & \varphi\left(\boldsymbol{x}_1\left(t_f\right), \boldsymbol{x}_2\left(t_f\right), t_f\right) + \int_0^{tf} L(\boldsymbol{x}_1(t), \boldsymbol{x}_2(t), u(t), t)\, dt \\ & + \int_0^{tf} \boldsymbol{\lambda}_1^T \left(\boldsymbol{G}(\boldsymbol{x}_1(t), \boldsymbol{x}_2(t), u(t), t) - \frac{d\boldsymbol{x}_1}{dt}\right) dt \\ & + \int_0^{tf} \boldsymbol{\lambda}_2^T \left(\boldsymbol{F}(\boldsymbol{x}_1(t), \boldsymbol{x}_2(t), u(t), t) - {}_0^C D_t^{\alpha} \boldsymbol{x}_2\right) dt \end{aligned} \tag{21}$$

As it was done with the vector of state variables, the vector or multipliers (also known as adjoint variables) is partitioned too. The multipliers for the ordinary differential equations are represented as $\boldsymbol{\lambda}_1$, whereas $\boldsymbol{\lambda}_2$ represents the vector of multipliers for the fractional differential equations.

By defining a fractional-ordinary Hamiltonian as:

$$H\left[\boldsymbol{x}_1(t), \boldsymbol{x}_2(t), \boldsymbol{\lambda}_1(t), \boldsymbol{\lambda}_2(t), u(t), t\right] = L + \boldsymbol{\lambda}_1^T \boldsymbol{G} + \boldsymbol{\lambda}_2^T \boldsymbol{F} \tag{22}$$

Eq. (21) can then be reformulated in terms of that function as follows:

$$\begin{aligned}\bar{J}(u) \quad = \quad & \varphi\left(\boldsymbol{x}_1\left(t_f\right), \boldsymbol{x}_2\left(t_f\right), t_f\right) \\ & + \int_0^{tf} \left[H\left(\boldsymbol{x}_1(t), \boldsymbol{x}_2(t), \boldsymbol{\lambda}_1(t), \boldsymbol{\lambda}_2(t), u(t), t\right)\right. \\ & \left. - \boldsymbol{\lambda}_1^T \frac{d\boldsymbol{x}_1}{dt} - \boldsymbol{\lambda}_2^T \, {}_0^C D_t^{\alpha} \boldsymbol{x}_2\right] dt \end{aligned} \tag{23}$$

Variational calculus is now applied to Eq. (23). The details of the derivation are provided in the supplementary information file. The results for the necessary optimality conditions are:

$$-\frac{d\boldsymbol{\lambda}_1}{dt} = \frac{\partial H}{\partial \boldsymbol{x}_1} = \frac{\partial L}{\partial \boldsymbol{x}_1} + \boldsymbol{\lambda}_1^T \frac{\partial \boldsymbol{G}}{\partial \boldsymbol{x}_1} + \boldsymbol{\lambda}_2^T \frac{\partial \boldsymbol{F}}{\partial \boldsymbol{x}_1} \tag{24}$$

$${}_t D_{t_f}^{\alpha} \boldsymbol{\lambda}_2 = \frac{\partial H}{\partial \boldsymbol{x}_2} = \frac{\partial L}{\partial \boldsymbol{x}_2} + \boldsymbol{\lambda}_1^T \frac{\partial \boldsymbol{G}}{\partial \boldsymbol{x}_2} + \boldsymbol{\lambda}_2^T \frac{\partial \boldsymbol{F}}{\partial \boldsymbol{x}_2} \tag{25}$$

$$\boldsymbol{\lambda}_1\left(t_f\right) = \frac{\partial \varphi}{\partial \boldsymbol{x}_1}\left(t_f\right) \tag{26}$$

$${}_t I_{t_f}^{1-\alpha} \boldsymbol{\lambda}_2\left(t_f\right) = \frac{\partial \varphi}{\partial \boldsymbol{x}_2}\left(t_f\right) \tag{27}$$

$$\frac{\partial H}{\partial u} = \frac{\partial L}{\partial u} + \boldsymbol{\lambda}_1^T \frac{\partial \boldsymbol{G}}{\partial u} + \boldsymbol{\lambda}_2^T \frac{\partial \boldsymbol{F}}{\partial u} = 0 \tag{28}$$

Eqs. (19), (20) and (24) through (28) represent the necessary optimality conditions for a generalized FOOCP. Equation (26) and (27) provide the end conditions for the ordinary and fractional multipliers. Eq. (28) allows the determination of the optimal profile for the control variable (expression commonly known as the control law). The result is a two-point boundary value problem. The expressions for the end conditions can be simpler; for instance, when the objective function is in Lagrangian form (that is, no scalar function φ appears it the objective function). In that case, since the terminal conditions for the multipliers are given in terms of the derivatives of φ with respect to the state variables, the end conditions for the multipliers are equal to zero.

Table 1 provides the fractional-ordinary optimality conditions derived in this work for the various forms of the objective function of the FOOCP. The optimality conditions are solved by an iterative procedure based on the gradient method which is explained in the following section.

3.3. Solving the optimality conditions of a FOOCP: a gradient method based approach

The numerical method for solving the optimality conditions used in this work is based on Poyntriagin Maximum Principle, which we apply by using the gradient method. We have modified the conventional gradient method, however, to consider the presence of fractional differential equations and fractional end conditions. The following is a summary of the algorithmic steps that we propose in our optimization strategy:

Step 1. Propose an initial feasible guess for the control variable profile $u(t) = u_0(t)$.

Step 2. Use the fractional-ordinary predictor-corrector technique to perform forward integration of the state equations (ordinary and fractional; Eqs. (19) and (20)) by using the known initial conditions. Time profiles are obtained for x_1 and x_2.

Step 3. Use the end conditions of the Lagrange multipliers λ_1 and λ_2 and the fractional-ordinary predictor-corrector technique to perform backward integration of Eqs. (24) and (25) to obtain the time profiles of those multipliers.

Step 4. Update the control variable profile. Using a gradient method-based approach, the new estimation is given by the following expression:

$$u_{k+1} = u_k - \varepsilon_k \left[\frac{\partial H}{\partial u}\right]_k$$

where ε_k is a scalar chosen for each particular problem; its definition generally implies trial and error. If the value is too small, the number of iterations needed grows significantly, but if it is too large, convergence might not be achieved. The derivative of the fractional ordinary Hamiltonian with respect to the control variable is given by Eq. (28).

Step 5. The algorithm returns to Step 2 and continues until the convergence criterion is met. The criterion might be in terms of sufficiently small values of either $[\frac{\partial H}{\partial u}]_k$or the difference $(u_{k+1} - u_k.)$

If the objective function is in either linear Mayer or Bolza forms (*i. e.* $\varphi \neq 0$), a numerical approximation to the end condition of the fractional multipliers, λ_2, is needed. The description of an algorithm to estimate that end condition is given in the supplementary information file accompanying this paper.

In summary, this section has described the three main numerical/theoretical tools used in our work. The FOPC method of Section 3.1 can be applied to simulate a SOFDE, but it is also a fundamental tool for the non-linear correlation of experimental data to determine fractional orders of the fractional differential equations and, as seen in Section 3.3, to support the algorithm for optimization. The generalized optimality conditions of Section 3.2 and the gradient method of Section 3.3 are together the main basis for our optimization approach. An additional contribution is given in the next section, as we suggest an approach to reformulate fractionalized dynamic systems.

4. Fractionalization of ordinary models and our reformulation approach

In compartmental modeling, as the name suggests, a complex system under analysis is divided into compartments. In particular, this modeling approach provides a framework to study the dynamics of materials flow (drugs, nutrients, etc.) among different compartments. Each compartment represents a group of components of the system with similar characteristics; a compartment can be either a conceptual or a physical region.

4.1. Fractionalization of an ordinary compartmental model

Dokoumetzidis et al. (2010a) explain that incorporating fractional behavior in some compartments of an ordinary multicompartmental model is not as simple as just assigning a fractional order to the derivatives in the left-hand side of the ordinary differential equations of the model; the authors show that such practice may produce inconsistent systems which violate mass balances. Therefore, they propose a formal fractionalization strategy so that a consistent fractional model can be derived from the ordinary model. Such strategy is applied to the case studies of this work.

As a brief summary, the fractionalization approach involves (please see Dokoumetzidis et al., 2010b):

(i) Integrating the ordinary differential equations to achieve a set of integral equations.
(ii) Modifying the kernel of the integral terms to appropriate functions in power-law form, so that the integral terms become Riemann–Liouville fractional integrals.
(iii) Taking the first derivative to each of the resulting equation so that the Riemann–Liouville fractional integrals become Riemann–Liouville fractional derivatives.

Table 1
Necessary optimality condition ordinary-fractional optimal control problems.

Objective function	Euler-Lagrange optimality conditions
$J(u) = \varphi(\boldsymbol{x}_1(t_f), \boldsymbol{x}_2(t_f), t_f) + \int_0^{tf} L(\boldsymbol{x}_1(t), \boldsymbol{x}_2(t), u(t), t)dt$	$-\frac{d\boldsymbol{\lambda}_1}{dt} = \frac{\partial H}{\partial \boldsymbol{x}_1} = \frac{\partial L}{\partial \boldsymbol{x}_1} + \boldsymbol{\lambda}_1^T \frac{\partial \boldsymbol{G}}{\partial \boldsymbol{x}_1} + \boldsymbol{\lambda}_2^T \frac{\partial \boldsymbol{F}}{\partial \boldsymbol{x}_1}$ $\boldsymbol{\lambda}_1(t_f) = \frac{\partial \varphi}{\partial \boldsymbol{x}_1}(t_f)$ ${}_tD_{t_f}^{\alpha}\boldsymbol{\lambda}_2 = \frac{\partial H}{\partial \boldsymbol{x}_2} = \frac{\partial L}{\partial \boldsymbol{x}_2} + \boldsymbol{\lambda}_1^T \frac{\partial \boldsymbol{G}}{\partial \boldsymbol{x}_2} + \boldsymbol{\lambda}_2^T \frac{\partial \boldsymbol{F}}{\partial \boldsymbol{x}_2}$ ${}_tI_{t_f}^{1-\alpha}\boldsymbol{\lambda}_2(t_f) = \frac{\partial \varphi}{\partial \boldsymbol{x}_2}(t_f)$ $\frac{\partial H}{\partial u} = \frac{\partial L}{\partial u} + \boldsymbol{\lambda}_1^T \frac{\partial \boldsymbol{G}}{\partial u} + \boldsymbol{\lambda}_2^T \frac{\partial \boldsymbol{F}}{\partial u} = 0$
$J(u) = \varphi(\boldsymbol{x}_1(t_f), \boldsymbol{x}_2(t_f), t_f)$	$-\frac{d\boldsymbol{\lambda}_1}{dt} = \frac{\partial H}{\partial \boldsymbol{x}_1} = \boldsymbol{\lambda}_1^T \frac{\partial \boldsymbol{G}}{\partial \boldsymbol{x}_1} + \boldsymbol{\lambda}_2^T \frac{\partial \boldsymbol{F}}{\partial \boldsymbol{x}_1}$ $\boldsymbol{\lambda}_1(t_f) = \frac{\partial \varphi}{\partial \boldsymbol{x}_1}(t_f)$ ${}_tD_{t_f}^{\alpha}\boldsymbol{\lambda}_2 = \frac{\partial H}{\partial \boldsymbol{x}_2} = \boldsymbol{\lambda}_1^T \frac{\partial \boldsymbol{G}}{\partial \boldsymbol{x}_2} + \boldsymbol{\lambda}_2^T \frac{\partial \boldsymbol{F}}{\partial \boldsymbol{x}_2}$ ${}_tI_{t_f}^{1-\alpha}\boldsymbol{\lambda}_2(t_f) = \frac{\partial \varphi}{\partial \boldsymbol{x}_2}(t_f)$ $\frac{\partial H}{\partial u} = \boldsymbol{\lambda}_1^T \frac{\partial \boldsymbol{G}}{\partial u} + \boldsymbol{\lambda}_2^T \frac{\partial \boldsymbol{F}}{\partial u} = 0$
$J(u) = \int_0^{tf} L(\boldsymbol{x}_1(t), \boldsymbol{x}_2(t), u(t), t)dt$	$-\frac{d\boldsymbol{\lambda}_1}{dt} = \frac{\partial H}{\partial \boldsymbol{x}_1} = \frac{\partial L}{\partial \boldsymbol{x}_1} + \boldsymbol{\lambda}_1^T \frac{\partial \boldsymbol{G}}{\partial \boldsymbol{x}_1} + \lambda_2^T \frac{\partial \boldsymbol{F}}{\partial \boldsymbol{x}_1}$ ${}_t^CD_{t_f}^{\alpha}\boldsymbol{\lambda}_2 = \frac{\partial H}{\partial \boldsymbol{x}_2} = \frac{\partial L}{\partial \boldsymbol{x}_2} + \boldsymbol{\lambda}_1^T \frac{\partial \boldsymbol{G}}{\partial \boldsymbol{x}_2} + \boldsymbol{\lambda}_2^T \frac{\partial \boldsymbol{F}}{\partial \boldsymbol{x}_2}$ $\boldsymbol{\lambda}_1(t_f) = \boldsymbol{\lambda}_2(t_f) = 0$ $\frac{\partial H}{\partial u} = \frac{\partial L}{\partial u} + \boldsymbol{\lambda}_1^T \frac{\partial \boldsymbol{G}}{\partial u} + \boldsymbol{\lambda}_2^T \frac{\partial \boldsymbol{F}}{\partial u} = 0$

(iv) Rewriting the Riemann–Liouville fractional derivatives as the equivalent Caputo fractional derivatives.

Once the fractionalization approach is applied to an ordinary model, each of the equations of the resulting system involves both ordinary and fractional derivative operators, so that the system can be considered as a linear multi-term set of FDEs. In the compartmental models used in this work, the units of the transfer rates among compartments in the fractionalized equations are consistent.

In the work of Dokoumetzidis et al. (2010b), given the form of the equations, the authors suggest rewriting the system in the Laplace domain and then using a numerical inverse Laplace transform algorithm to simulate the system. The approach proposed in this paper does not apply such transformation. Instead, a reformulation of the linear multi-term FDEs allows the use of the numerical tools developed in this work. The reformulation is described in the following subsection.

4.2. Proposed reformulation of a fractional model

The main step of the reformulation approach involves the incorporation of artificial variables to represent the fractional derivatives of the original state variables. Consider a simple set of liner multi-term FDEs of the form ($0 < \alpha < 1$):

$$\frac{dx_{11}}{dt} + \lambda_1 \ {}_0^CD_t^{1-\alpha}x_{21} = f_1(\boldsymbol{x}, t) \tag{29}$$

$$\frac{dx_{21}}{dt} + \lambda_2 \ {}_0^CD_t^{1-\alpha}x_{21} = f_2(\boldsymbol{x}, t) \tag{30}$$

That kind of equations is commonly found when the fractionalization approach of the previous subsection is applied to an ordinary model. The first idea is introducing a new variable for each fractional term involved in the equations. Hence, by defining $x_{22}(t) = {}_0^CD_t^{1-\alpha}x_{21}$, where $x_{22}(0) = 0$, Eqs. (29) and (30) are reformulated as a fractional-ordinary system:

$${}_0^CD_t^{1-\alpha}x_{21} = x_{22}$$

$$\frac{dx_{11}}{dt} = f_1(\boldsymbol{x}, t) - \lambda_1 \ x_{22}$$

$$\frac{dx_{21}}{dt} = f_2(\boldsymbol{x}, t) - \lambda_2 \ x_{22}$$

As a second step, the reformulation requires an expression to estimate the time dependent behavior of the artificial variable x_{22}. That is obtained by using both the original state equation of variable x_{21} and the commutative property of fractional derivation given by Eq. (3). Recall that, in Eq. (3), α and β are arbitrary constants; also, when the fractional order of a fractional derivative is integer, the fractional derivative reduces to an ordinary derivative. The outcome of this step is as follows:

$$\frac{dx_{21}}{dt} = {}_0^CD_t^1x_{21} = {}_0^CD_t^{\alpha+(1-\alpha)}x_{21} = {}_0^CD_t^{\alpha}\left({}_0^CD_t^{1-\alpha}x_{21}\right) = {}_0^CD_t^{\alpha}x_{22}$$

Therefore, the system of equations becomes:

$${}_0^CD_t^{1-\alpha}x_{21} = x_{22} \tag{31}$$

$$\frac{dx_{11}}{dt} = f_1(\boldsymbol{x}, t) - \lambda_1 \ x_{22} \tag{32}$$

$${}_0^CD_t^{\alpha}x_{22} = f_2(\boldsymbol{x}, t) - \lambda_2 \ x_{22} \tag{33}$$

The significance of this reformulation is that the set of multi-term FDEs becomes a SFODE, which can be approached by using

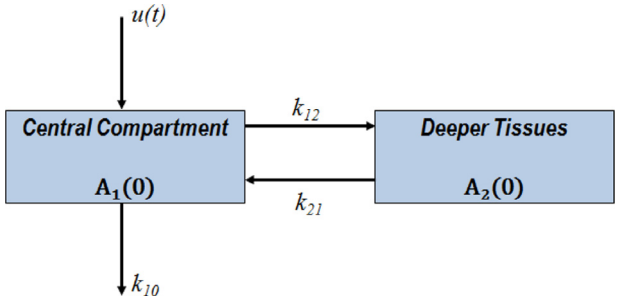

Fig. 1. Compartmental model for Amiodarone distribution.

the tool proposed in this work. Garrapa (2018) discusses and alternative approach to solve multi-term FDES through a numerical algorithm to integrate FDEs.

5. Case studies

We selected two case studies whose models, simulations and optimal results were previously reported in the literature. Recent research efforts (Copot et al, 2017a; Copot et al, 2017b; Ionescu and Kelly, 2017) shows that the modeling of drug absorption, distribution and elimination within the body has to consider *anomalous* phenomena caused by drug trapping and tissue heterogeneity. The models of the case studies consider some of those issues but do not implement some of that current knowledge about the modeling of biological phenomena through fractional calculus. Nevertheless, we are keeping the models as they were reported for two reasons. Firstly, their mathematical nature results (through the reformulation that we propose) in a fractional-ordinary model (and fractional-ordinary optimal control if a performance index is included), which is the main focus of this work; secondly, they could help us assess the performance of our methods by direct comparison. The description of the models and the reformulation as SFODE are provided here.

5.1. A Compartmental model in pharmacokinetics: administration and absorption of amiodarone

The first case-study involves the administration and distribution of the drug amiodarone within the body. It is a simple example, but it involves all of the elements needed to clearly illustrate our approach. Amiodarone is a drug used to prevent and treat various types of irregular heartbeats; it has serious side effects include lung toxicity, as well as liver, vision and thyroid problems. A pharmacokinetics compartmental model has been provided by Dokoumetzidis et al. (2010b). The formulation suggested by such authors is derived as follows.

5.1.1. Ordinary model for the amiodarone case-study

Fig. 1 provides a schematic representation of a compartmental model for Amiodarone pharmacokinetics proposed by Dokoumetzidis et al. (2010b). The system considers a central compartment to represent perfused tissues and general circulation as well as a peripheral compartment used for representing deeper tissues. The processes of interest include mass transfer from the central to the peripheral compartment, mass elimination from the central compartment and a mass flux from the peripheral to the central compartment.

Assuming first order dynamics for all of the mass transfer processes, mass balances for each compartment result in:

$$\frac{dA_1}{dt} = -k_{12}A_1(t) + k_{21}A_2(t) - k_{10}A_1(t) + u(t) \tag{34}$$

$$\frac{dA_2}{dt} = k_{12}A_1(t) - k_{21}A_2(t) \tag{35}$$

where $A_1(t)$ and $A_2(t)$ represent the masses of the drug in each compartment and the various k_{ij} represent the mass transfer rates between the compartments or the elimination rate. $u(t)$ is the input rate from the drug to the central compartment.

5.1.2. Fractionalization of the model for the amiodarone case-study

Applying the fractionalization strategy of Section 4.1 to Eqs. (34) and (35), the expressions are reformulated as:

$$\frac{dA_1}{dt} = -(k_{12}+k_{10})A_1 + k_{21}\,{}_0^C D_t^{1-\alpha} A_2 + u(t) \tag{36}$$

$$\frac{dA_2}{dt} = k_{12}A_1 - k_{21}\,{}_0^C D_t^{1-\alpha} A_2 \tag{37}$$

The fractionalization assumes that the mass transfer from the peripheral compartment (deeper tissues) to the central compartment (general circulation) follows anomalous fractional behavior (the corresponding rate constant is k_{21}). Notice that -Eqs. (36)–(37) involve both ordinary and fractional derivative operators. The units of the variables and parameters are as follows: units of mass for A_1 and A_2; $time^{-\alpha}$ for k_{21}; $time^{-1}$ for $k_{12}$and k_{10}; *mass/time* for u. Following the discussions presented by Dokoumetzidis et al. (2010b), the units of the rate constant k_{21} ($time^{-\alpha}$) are consistent with the slower kinetics arising as a result of the (non-exponential) power-law nature of the fractional derivative in Eq. (36). This slower kinetics will eventually lead to drug accumulation at long administration times; such a behavior is consistent with drug trapping in biological tissues.

5.1.3. Proposed reformulation of the fractional model for the amiodarone case-study

When the reformulation approach of Section 4.2 is applied to Eqs. (36) and (37), a new artificial variable $B(t)$ is defined as $B(t) = {}_0^C D_t^{1-\alpha} A_2$, where $B(0) = 0$. As a consequence of the definition, units of B are $mass/time^{1-\alpha}$.

The result is:

$${}_0^C D_t^{1-\alpha} A_2 = B \tag{38}$$

$$\frac{dA_1}{dt} = -(k_{12}+k_{10})A_1 + k_{21}B + u(t) \tag{39}$$

$$\frac{dA_2}{dt} = k_{12}A_1 - k_{21}B \tag{40}$$

Eq. (38) provides the dynamics of A_2 and Eq. (39) the dynamics of A_1. The dynamics of $B(t)$ is obtained by applying Eq. (3) to the derivative of Eq. (40):

$$\frac{dA_2}{dt} = {}_0^C D_t^1 A_2 = {}_0^C D_t^{\alpha+(1-\alpha)} A_2 = {}_0^C D_t^{\alpha}\left({}_0^C D_t^{1-\alpha} A_2\right) = {}_0^C D_t^{\alpha} B$$

Given the previous identity, it is important to notice that units of both $\frac{dA_2}{dt}$ and ${}_0^C D_t^{\alpha} B$ are *mass/time*.The final result is the SFODE given by Eqs. (41) through (43).

$${}_0^C D_t^{1-\alpha} A_2 = B \tag{41}$$

$$\frac{dA_1}{dt} = -(k_{12}+k_{10})A_1 + k_{21}B + u(t) \tag{42}$$

$${}_0^C D_t^{\alpha} B = k_{12}A_1 - k_{21}B \tag{43}$$

The equations of the system are no longer multi-term FDEs. Instead, the system includes now one ordinary differential equation and two fractional differential equations and, therefore, it

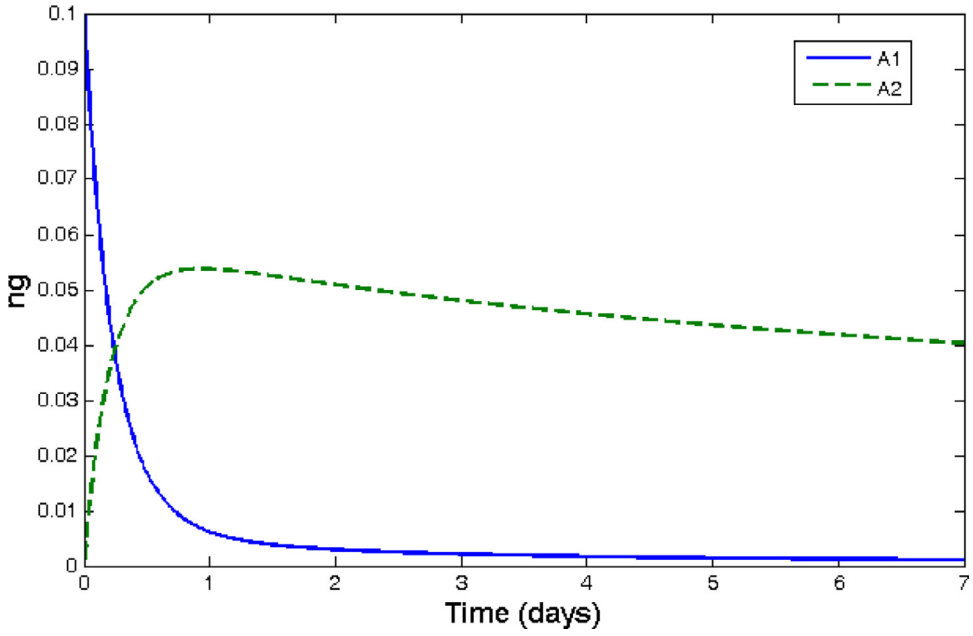

Fig. 2. Amiodarone mass in the central (A1) and peripheral (A2) compartments after an initial dose of 0.1 ng.

can be integrated directly with the FOPC method explained in Section 3.1. Fig. 2 shows the profiles of amiodarone during seven days in the central and peripheral compartments obtained by the numerical integration. The model parameters suggested by Dokumetzidis et al. (2010b) are used in this work; the values are $\alpha = 0.5870$, k_{10}=1.4913 day^{-1}, $k_{12} = 2.9522$ day^{-1} and $k_{21} = 0.4854$ day$^{-\alpha}$. Amiodarone accumulates in deep tissues; in fact, if the simulation of the model continues further in time, it can actually show that, after thirty days of the initial dose of 0.1 ng, its amount in the blood plasma is basically zero, but a significant amount (about 0.024 ng) can still be found in the peripheral compartment. The fractional ordinary model will be further studied to evaluate our approach to solve FOOCPs in Section 6.

5.2. A thermal hydrolysis: production of mezcal from agave

The ordinary model of this example has been taken from the work of Garcia-Soto et al (2011). The fractional calculus approach was reported by Toledo-Hernandez et al. (2014a).

As pointed out by Toledo-Hernandez et al. (2014a), the ordinary differential equations of the ordinary model are quite simple and fractional calculus might not represent a significant modeling advantage in this case. However, those authors use that example to explain the fractionalization technique described in Section 4.1. We also use this case-study since, besides the fractionalization strategy, literature provides optimization (optimal control) results obtained by an iterative approach based on the discretization of the time intervals.

This case represents the thermal treatment of fructans (from *Agave salmiana*) as the first step in mezcal production given by the following reaction (Garcia-Soto et al, 2011):

$$Fructans \xrightarrow{k_h} \begin{bmatrix} Fructose \\ Glucose \\ other \end{bmatrix} Reducing\ Sugars$$

$$\xrightarrow{k_d} \begin{bmatrix} Furfural \\ 5-(hydroxymethyl)furfural \\ other \end{bmatrix} Furans$$

The fructans (P) are hydrolyzed into reducing sugars; the sugars further undergo partial degradation to form furans (D). The rate constants of hydrolysis and degradation are k_h and k_d, respectively. The ordinary and the fractionalized models were reported by Toledo-Hernandez et al. (2014a) and are provided in the supplementary information file which accompanies this manuscript.

5.2.1. Reformulation as a SFODE

In this case, the reformulation of the fractionalized model requires the definition of two artificial variables (two new fractional differential equations). The resulting SFODE for this example includes four fractional differential equations and one ordinary differential equation.

$${}_0^C D_t^{1-\alpha_1} P(t) = X \tag{44}$$

$${}_0^C D_t^{1-\alpha_2} M(t) = Y \tag{45}$$

$${}_0^C D_t^{\alpha_1} X = -k_h \left[X + P(0) \frac{t^{\alpha_1 - 1}}{\Gamma(\alpha_1)} \right] \tag{46}$$

$${}_0^C D_t^{\alpha_2} Y = k_h \left[X + P(0) \frac{t^{\alpha_1 - 1}}{\Gamma(\alpha_1)} \right] - k_d \left[Y + M(0) \frac{t^{\alpha_2 - 1}}{\Gamma(\alpha_2)} \right] \tag{47}$$

$$\frac{dD}{dt} = k_d \left[Y + M(0) \frac{t^{\alpha_2 - 1}}{\Gamma(\alpha_2)} \right] \tag{48}$$

Initial conditions are given by $P(0) = P_0$, $M(0) = M_0$, $D(0) = D_0$, $X(0) = 0$ and $Y(0) = 0$. Experimental data and the time profiles obtained in this work are shown in Fig. 3; the numerical integration of Eqs. (44) through (48) was done by using our implementation of the FOPC method described before. Results are basically the same as those reported by Toledo-Hernandez et al. (2014a) that used Laplace transformation for the simulations. Table 2 shows the model parameters used for both the simulation of Fig. 3 and the optimization problem described in the following section.

6. Optimization of the SFODE: formulating and solving the FOOCP

To illustrate the use of the optimality conditions and the optimization strategy proposed in Section 3, the fractional ordinary

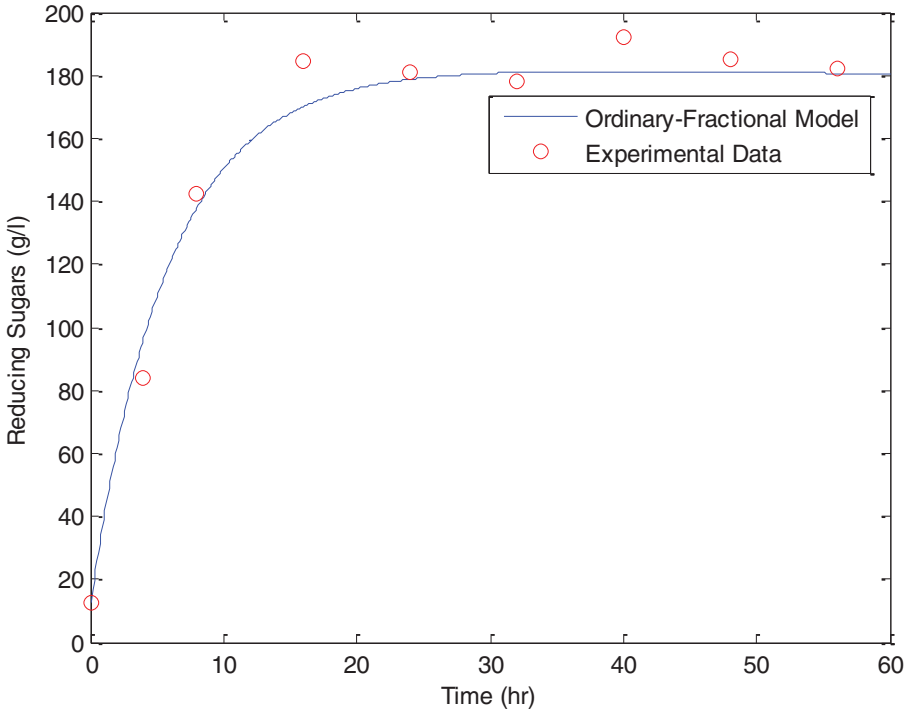

(a)

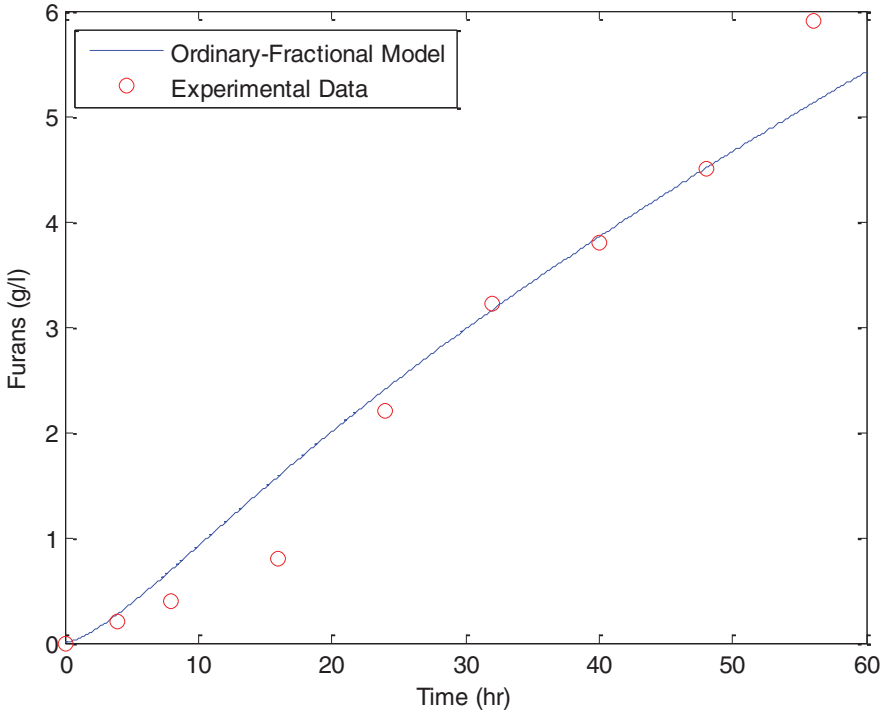

(b)

Fig. 3. Time profiles of reducing sugars (a) and furans (b). Experimental values are compared against the integration of the SFODE of the fractional model by the FOPC method.

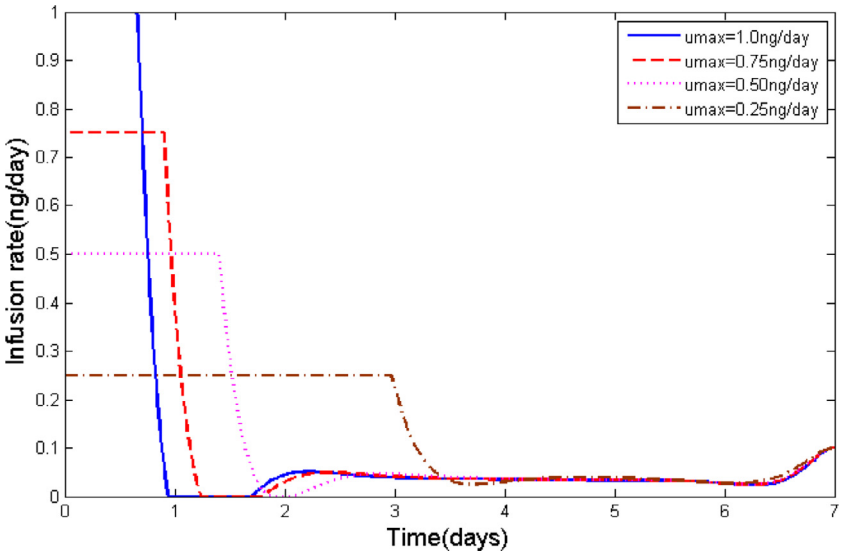

Fig. 4. Optimal infusion rate of amiodarone.

Table 2
Model parameter for the thermal hydrolysis fractional model.

Temperature= 96°C	Temperature= 106°C
$\alpha_1 = 0.9738$	$\alpha_1 = 0.9738$
$\alpha_2 = 0.7448$	$\alpha_2 = 0.7448$
$k_h = 0.0552\ h^{-\alpha_1}$	$k_h = 0.1729\ h^{-\alpha_1}$
$k_d = 5.0789\ x\ 10^{-4}\ h^{-\alpha_2}$	$k_d = 0.0014\ h^{-\alpha_2}$

models formulated and simulated in the previous section are now modified to conform fractional-ordinary optimal control problems; the derivations and optimization results involved in each of the examples are described next.

6.1. Administration and absorption of amiodarone

In the first example, the objective is to achieve and maintain the necessary amount of amiodarone in compartment 2 (deeper tissues), A_2, and, at the same time, to avoid reaching the amount at which the drug becomes toxic to the organism. Herceg et al. (2017) address a similar problem, considering specific discrete doses every half a day for seven days. The corresponding FOOCP used in this work is given by Eqs. (49) through (54).

$$Minimize\ J = \int_0^{t_f} (A_2(t) - \delta)^2 dt \tag{49}$$

Subject to the SOFDE derived previously and the bounds of the variables:

$${}_0^C D_t^{1-\alpha} A_2 = B \tag{50}$$

$$\frac{dA_1}{dt} = -(k_{12} + k_{10})A_1 + k_{21}B + u(t) \tag{51}$$

$${}_0^C D_t^{\alpha} B = k_{12}A_1 - k_{21}B \tag{52}$$

$$A_1,\ A_2 \leq \theta \tag{53}$$

$$0 \leq u \leq u_{max} \tag{54}$$

where δ is the target amount of A_2; θ is the toxicity bound for the amiodarone and u_{max} is the maximum allowable dose. Initial conditions are $A_1(0) = A_2(0) = B(0) = 0$. The goal is to find the optimal values of the drug infusion rates represented by $u(t)$.

6.1.1. Euler Lagrange optimality conditions

From the previous SFODE, the fractional-ordinary Hamiltonian is defined as:

$$H = (A_2 - \delta)^2 + B\lambda_1 + (-(k_{12} + k_{10})A_1 + k_{21}B + u(t))\lambda_2 + (k_{12}A_1 - k_{21}B)\lambda_3$$

The optimality conditions derived from the Hamiltonian are:

$${}_t^C D_{t_f}^{1-\alpha} \lambda_1 = \frac{\partial H}{\partial A_2} = 2(A_2 - \delta) \tag{55}$$

$$-\frac{d\lambda_2}{dt} = \frac{\partial H}{\partial A_1} = -(k_{12} + k_{10})\lambda_2 + k_{12}\lambda_3 \tag{56}$$

$${}_t^C D_{t_f}^{\alpha} \lambda_3 = \frac{\partial H}{\partial B} = \lambda_1 + k_{21}\lambda_2 - k_{21}\lambda_3 \tag{57}$$

The objective function is in Lagrangian form, so that $\lambda_1(t_f) = \lambda_2(t_f) = \lambda_3(t_f) = 0$ and the Caputo definitions of fractional derivatives are used directly. Finally, the control law is:

$$\frac{\partial H}{\partial u} = \lambda_2 = 0$$

The two-point boundary value problem is defined then by -(Eqs. (50)–(54) and -(Eqs. (55)–(57) as well as by the initial conditions of the state variables, the end conditions of the multipliers and the control law. Notice that the units of all of the terms of the Hamiltonian as well as those of Eqs. (55)–(57) are consistent. Recall that the units of the original variables and parameters are: units of mass for A_1 and A_2; $time^{-\alpha}$ for k_{21}; $time^{-1}$ for $k_{12}$and k_{10}; *(mass/time)* for u; units of B are $(mass/time^{1-\alpha})$. Further, the units of the new adjoint variables are $(mass\ time^{1-\alpha})$ for λ_1, *(mass time)* for λ_2, and *(mass time)* for λ_3. In that way, the units of all of the terms of the Hamiltonian are $(mass^2)$; the units of all of the terms of Eqs. (55) and (56) are units of *(mass)*; finally, the units of all of the terms of Eq. (57) are $(mass\ time^{1-\alpha})$.

6.1.2. Solving the Euler Lagrange optimality conditions with the gradient method

The system can be solved by using the gradient method proposed in this paper. The values used for the modeling parameters are $\delta = 0.4ng$ and $\theta = 0.5ng$; further, four cases of the maximum allowable dose were considered, $u_{max} = [1.0,\ 0.75,\ 0.5,\ 0.25]\ ng/day$. Fig. 4, Fig. 5 and Fig. 6 show the optimal infusion rates and the amounts of amiodarone in both of the

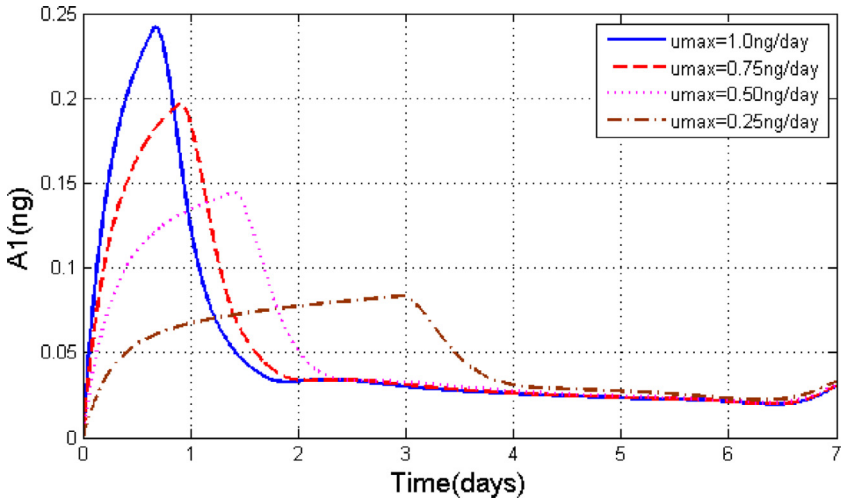

Fig. 5. Optimal profile of amiodarone in the central compartment.

compartments. The results for the control variable represent a continuous administration route for the amiodarone which, in principle, would require a continuous infusion device that can provide the appropriate variable amounts of drug during the entire time interval. The optimal profiles present a similar trend. The infusion rate starts at the maximum allowable dose until the target amount of drug in the tissues is achieved. Then, the infusion rate rapidly decreases and is kept at lower values, but still maintaining the mass of amiodarone at the appropriate target level $\delta = 0.4ng$. The maximum allowable dose is related to the time period required to reach the target; as u_{max} increases, the time needed decreases. That is also consistent with a decrease in the objective function.

6.1.3. Practical considerations for the administration of amiodarone: treatment based on discrete doses

For practical purposes in this particular example, notice that a continuous administration of the drug cannot be undertaken for long periods of time. In such case, it is generally preferred to provide specific doses of the drug in particular discrete points in time during the treatment. That issue will be addressed in this section.

In such case, the goal is to determine the optimal amount of drug to be administrated during finite periods of time of length Δt within the whole time interval. Let us define $n+1$ time points t_i $(i = 0, 1, 2, \ldots, n)$ t_i in the time interval $[t_0,\ t_f]$, where the time periods are defined as $\Delta t = t_{i+1} - t_i$.

As the first step in the approach, the continuous optimal profile, $u^*(t)$, as the one estimated in the previous section, is integrated along each of the time periods; the idea is to calculate the total amount of amiodarone to be administered at each period, d_i:

$$d_i = \int_{t_i}^{t_{i+1}} u^*(t)dt$$

An additional assumption in this section is that the total dose to be administrated in each period, d_i, will be provided at the beginning of the period, in t_i. Notice that the doses d_i are inputs to compartment 1 and affect directly the ordinary dynamics of variable A_1; nevertheless, the values of A_1 will indirectly affect the fractional dynamics of A_2 because of the coupling among the differential equations. Also notice that the estimation of d_i must consider that the behavior of the system variables is fractional.

Our study was conducted for three different administration routes, involving a time interval of seven days and constant time periods of Δt equal to 6, 12 and 24 h; that is $\Delta t = 0.25,\ 0.5$ *and* 1 days. The results for time periods of 12 h are presented in detail here, since the work by Herceg et al. (2017) consider such administration route; the rest of results are provided as supplementary material. Table 3 presents the doses administrated every 12 h for each of the four cases of Figs. 4–6 (four values of the maximum allowable infusion rate u_{max}). The discrete doses of Table 3 were estimated by using the optimal infusion rates of Fig. 4. The profiles of the amount of amiodarone in each of the compartments are shown in Figs. 7 and 8. Notice that the target value in compartment 2 is achieved from day 1 with small variations during the seven days of the administration of the drug. As a validation of the results, analogous profiles were obtained by Herceg et al. (2017) for an administration route which is similar as the ones defined in this work; their numerical approach is quite different though, since they use a rational approximation to the fractional derivatives.

Table 4 shows the value of the objective function $J = \int_0^{t_f} (A_2(t) - \delta)^2 dt$ obtained for the different values of the maximum allowable infusion rate. The three administration routes are shown for comparison purposes. For $\Delta\tau = 1$ day and $u_{max} > 0.5$, occurs that $d_0 > \theta$ and $A_1(0) > \theta$; therefore, no feasible solutions are achieved in those cases.

As a final note, it is important to emphasize that there is no limitation on the length of the time interval used for discrete dosage; the intervals can be constant, as in the previous results, or estimated otherwise so that the administration route considers any anomalous effect, such as the dynamics of molecular binding during the drug diffusion. Ionescu et al. (2016) show that equidistant discrete dosages can lead to drug accumulation within the body; therefore, in order to avoid harmful overdosing, (non-linear) logarithmic time-spaced dosages can be administered. To illustrate this issue, Fig. 9 shows the amounts of amiodarone in compartment 2 for two different discrete dosing time periods using u_{max}=0.5; one curve corresponds to a constant discrete dosing time period of $\Delta\tau$=0.5 days; in the other curve, the dosing time period was estimated by the non-linear expression $t_i = ({t_{i-1}}^{\alpha} + \alpha\Delta\tau^{\alpha})^{1/\alpha}$ with $\Delta\tau$=0.5 suggested by Hennion and Hanert (2013). In any case, the discrete doses are estimated by using the corresponding optimal continuous infusion profile as the one shown in Fig. 4.

6.2. Thermal hydrolysis

This section describes the optimization results for the fractional-ordinary model representing the thermal hydrolysis used in mezcal production. To incorporate the effect of temperature,

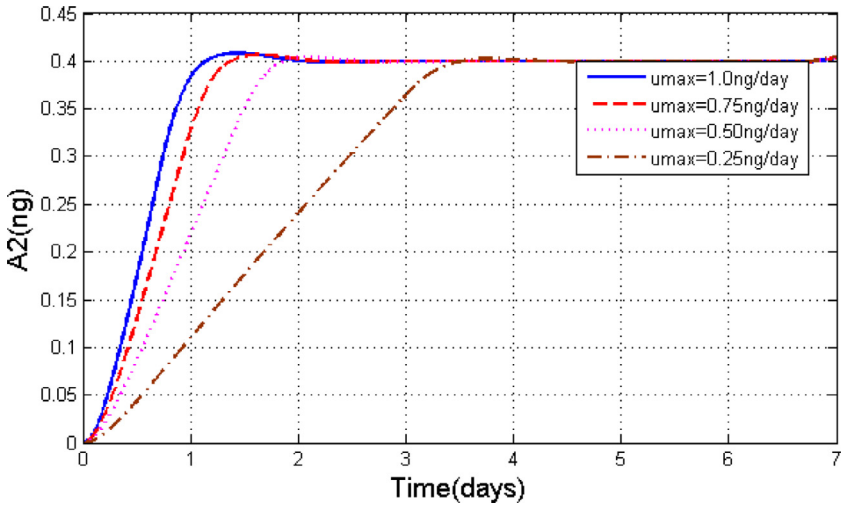

Fig. 6. Optimal profile of amiodarone in the peripheral compartment.

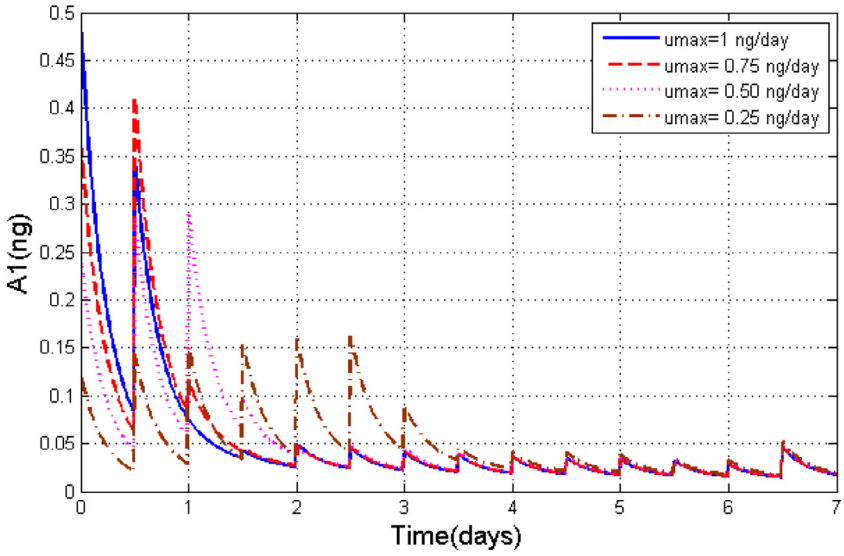

Fig. 7. Amiodarone in compartment 1 for an administration route of doses every 12 h.

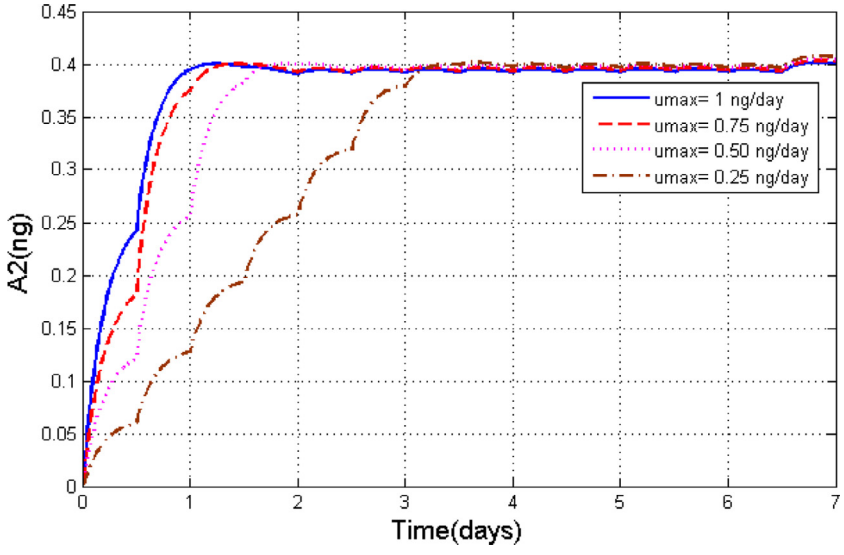

Fig. 8. Amiodarone in compartment 2 for an administration route of doses every 12 h.

Table 3
Doses (ng) provided every 12 h estimated with the optimal infusion rates.

Time (days)	Doses $u_{max} = 1$ ng/day	Doses $u_{max} = 0.75$ ng/day	Doses $u_{max} = 0.50$ ng/day	Doses $u_{max} = 0.25$ ng/day
0	0.4900	0.3675	0.2450	0.1225
0.50	0.2657	0.3515	0.2450	0.1225
1.0	0.0000	0.0355	0.2353	0.1225
1.50	0.0074	0.0029	0.0330	0.1225
2.0	0.0241	0.0218	0.0080	0.1225
2.50	0.0207	0.0220	0.0218	0.1224
2.0	0.0183	0.0189	0.0211	0.0479
3.50	0.0177	0.0178	0.0185	0.0133
3.0	0.0170	0.0172	0.0173	0.0173
4.50	0.0163	0.0166	0.0170	0.0194
5.0	0.0161	0.0163	0.0167	0.0181
5.50	0.0149	0.0148	0.0149	0.0150
6.0	0.0123	0.0125	0.0129	0.0150
6.50	0.0314	0.0321	0.0327	0.0354

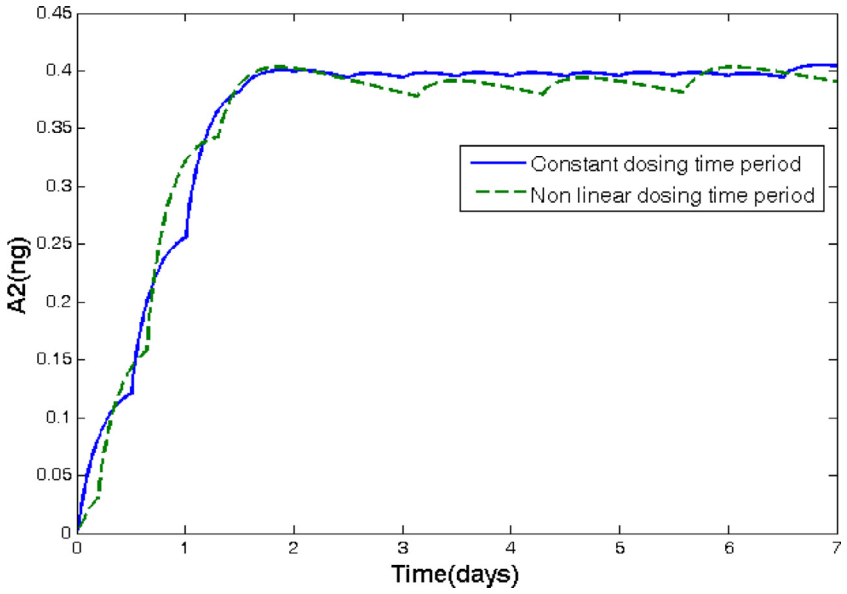

Fig. 9. Amiodarone in compartment 2 for linear ($\Delta\tau$=0.5 days) and nonlinear dosing time periods.

Table 4
Objective function of the FOOCP for the different administration routes

$u_{max}\,(ng/day)$	$\Delta\tau = 0.25\ days$	$\Delta\tau = 0.5\ days$	$\Delta\tau = 1\ day$
1.0	4.7696	3.1400	-
0.75	6.1829	4.3692	-
0.50	8.9611	7.0141	4.0242
0.25	17.3172	15.1182	11.5182

Arrhenius-like expressions are considered in the kinetics constants of the reactions:

$$k_h = k_1 e^{(-E_1/T)}$$

$$k_d = k_2 e^{(-E_2/T)}$$

The values of the constants k_1, k_2, E_1 and E_2 are estimated from experimental data provided by (Garcia-Soto et al, 2011). To approach the optimization of the system, the objective is defined as the maximization of the final concentration of reducing sugars, since they participate directly in the alcoholic fermentation to obtain mezcal; temperature is defined as the control variable. The same considerations were used by Toledo-Hernandez et al. (2014b). The FOOCP developed here is:

$$Minimize\ J = -M(t_f) \tag{58}$$

Subject to:

$${}_0^C D_t^{1-\alpha_1} P(t) = X \tag{59}$$

$${}_0^C D_t^{1-\alpha_2} M(t) = Y \tag{60}$$

$${}_0^C D_t^{\alpha_1} X = -k_1 e^{(-A_1/T)} \left[X + P(0) \frac{t^{\alpha_1 - 1}}{\Gamma(\alpha_1)} \right] \tag{61}$$

$${}_0^C D_t^{\alpha_2} Y = k_1 e^{(-A_1/T)} \left[X + P(0) \frac{t^{\alpha_1 - 1}}{\Gamma(\alpha_1)} \right] - k_2 e^{(-A_2/T)} \left[Y + M(0) \frac{t^{\alpha_2 - 1}}{\Gamma(\alpha_2)} \right] \tag{62}$$

$$\frac{dD}{dt} = k_2 e^{(-A_2/T)} \left[Y + M(0) \frac{t^{\alpha_2 - 1}}{\Gamma(\alpha_2)} \right] \tag{63}$$

$$369.15 \leq T \leq 379.15 \tag{64}$$

The bounds of the temperature are defined based on the data provided by Garcia-Soto et al. (2011).

6.2.1. The Euler-Lagrange optimality conditions for the thermal hydrolysis

The fractional-ordinary Hamiltonian function is given by:

$$H = X\lambda_1 + Y\lambda_2 - k_1 e^{(-A_1/T)}\left[X + P(0)\frac{t^{\alpha_1-1}}{\Gamma(\alpha_1)}\right]\lambda_3 + \left\{k_1 e^{(-A_1/T)}\left[X + P(0)\frac{t^{\alpha_1-1}}{\Gamma(\alpha_1)}\right] - k_2 e^{(-A_2/T)}\left[Y + M(0)\frac{t^{\alpha_2-1}}{\Gamma(\alpha_2)}\right]\right\}\lambda_4 + k_2 e^{(-A_2/T)}\left[Y + M(0)\frac{t^{\alpha_2-1}}{\Gamma(\alpha_2)}\right]\lambda_5 \quad (65)$$

Therefore, the differential expressions and the end conditions for the multipliers are given by -(Eqs. (66)–(70).

$${}_tD_{t_f}^{1-\alpha_1}\lambda_1(t) = \frac{\partial H}{\partial P} = 0 \qquad \lambda_1(t_f) = 0 \quad (66)$$

$${}_tD_{t_f}^{1-\alpha_2}\lambda_2(t) = \frac{\partial H}{\partial M} = 0 \qquad {}_tD_{t_f}^{1-\alpha_2}\lambda_2(t_f) = -1 \quad (67)$$

$${}_tD_{t_f}^{\alpha_1}\lambda_3(t) = \frac{\partial H}{\partial X} = \lambda_1 - k_1 e^{(-A_1/T)}\lambda_3 + k_1 e^{(-A_1/T)}\lambda_4 \qquad \lambda_3(t_f) = 0 \quad (68)$$

$${}_tD_{t_f}^{\alpha_2}\lambda_4(t) = \frac{\partial H}{\partial Y} = \lambda_2 - k_2 e^{(-A_2/T)}\lambda_4 + k_2 e^{(-A_2/T)}\lambda_5 \qquad \lambda_4(t_f) = 0 \quad (69)$$

$$\frac{d\lambda_5(t)}{dt} = \frac{\partial H}{\partial D} = 0 \qquad \lambda_5(t_f) = 0 \quad (70)$$

The two point boundary value problem consists of a SFODE defined by -(Eqs. (59)–(64) and (66)-(70). The initial conditions are $P(0) = P_0$, $M(0) = M_0$, $D(0) = D_0$, $X(0) = 0$ and $Y(0) = 0$. A simplification can be made previous to the numerical solution. By using Eqs. (66) and (70), one can show that $\lambda_5(t) = 0$ and $\lambda_1(t) = 0$. Finally, the expression for the control law is given by Eq. (71); the result $\lambda_5(t) = 0$ has already been applied:

$$\frac{\partial H}{\partial T} = -\frac{A_1}{T^2}k_1 e^{(-A_1/T)}\left[X + P(0)\frac{t^{\alpha_1-1}}{\Gamma(\alpha_1)}\right]\lambda_3 + \left\{\frac{A_1}{T^2}k_1 e^{(-A_1/T)}\left[X + P(0)\frac{t^{\alpha_1-1}}{\Gamma(\alpha_1)}\right] - \frac{A_2}{T^2}k_2 e^{(-A_2/T)}\left[Y + M(0)\frac{t^{\alpha_2-1}}{\Gamma(\alpha_2)}\right]\right\}\lambda_4 = 0 \quad (71)$$

The numerical approach based on the gradient method (Section 3.3) is used to obtain the solution to the FOOCP. The optimal value of the objective function is 181.6886 g/l. Fig. 10 shows the optimal temperature profile. Fig. 11 shows the results for the state variables. Toledo-Hernandez et al. (2014b) addressed the same problem. However, their approach was significantly different, since they used a method based on the Laplace transformation, the shooting method and non-linear programming techniques. Since Laplace transformation requires the system to be linear, Toledo-Hernandez et al. (2014b) divided the time interval in several time periods. Then, they assumed that the temperatures remain as constant in each time period, so that they can assume a linear behavior in each of such periods. Their result is therefore a step-wise profile, obtaining an optimal value of temperature to be kept in each of the time periods. In this work, no transformation is required; further, the non-linearity of the expressions does not impose a limitation to the approach. Further, a continuous optimal profile is achieved. Nevertheless, for this example, the optimal profiles of the state variables obtained by using our continuous temperature profile are not significantly different from those obtained with the step-wise temperature profile of Toledo-Hernandez et al. (2014b).

7. Summary and conclusions

Fractional calculus operators allow representing the dynamic behavior of variables that show memory effects. Generalized dynamic models, however, are expected to involve not only state variables that can be represented by fractional operators, but also variables that are better represented by conventional ordinary dynamics. In this context, our work describes conceptual and numerical tools that can be used for the modeling, simulation and optimization of systems that include both fractional and ordinary differential equations.

On the one hand, the most relevant aspects and developments of this work are:

(i) As a direct extension of the predictor corrector techniques used for the integration of either ordinary or fractional differential equations, a combined approach is implemented in this work, so that the predictor-corrector method simultaneously can handle both types of equations in the same dynamic model. Such integration technique has proven to be a fundamental tool for the simulation and optimization problems addressed in the case studies. Although a purely fractional integration method could be applied for the integration of both integer and fractional differential equations, the use of a fractional technique for the integration of an ordinary equation is not practical, since the computational effort increases unnecessarily. Therefore, the main contribution of the method developed here lies basically on the decomposition of the equations and on the numerical implementation of the strategy. As described, the fundamentals of this technique and other multi-step methods have already been reported in the literature (Garrapa, 2018).

(ii) A conceptually consistent approach to fractionalize ordinary models (Dokoumetzidis et al., 2010b) results in systems of linear multi-term FDEs that include both fractional and ordinary differential operators in the same equations. The reformulation approach used in this work allows the separation of the differential operators, so that a set of fractional-ordinary differential equations is obtained (only one operator in each equation). This reformulation is straightforward but significant, since it allows the use of the generalized predictor-corrector method and the optimization strategy developed in this work to address fractional-ordinary optimal control problems.

(iii) A generalized version of the Euler-Lagrange optimality conditions for fractional ordinary optimal control problems is provided in this work, so that the optimization of the combined problem can be solved through a gradient based approach. The expressions obtained for the generalized conditions are based on the derivations provided by Agrawal (2004, 2008) and on the classical theory of optimal control (Stengel, 1994).

(iv) Two case studies reported in the literature are used to validate our results. Previous solution approaches for both examples suggest the use or transformation methods to simulate and optimize the systems. Our approach represents and alternative that does not require such transformation to obtain the solution.

(v) For the thermal hydrolysis case study, a comparison with the approach used for Toledo-Hernandez et al. (2014b) shows that the numerical advantages of not using an inverse Laplace trans-

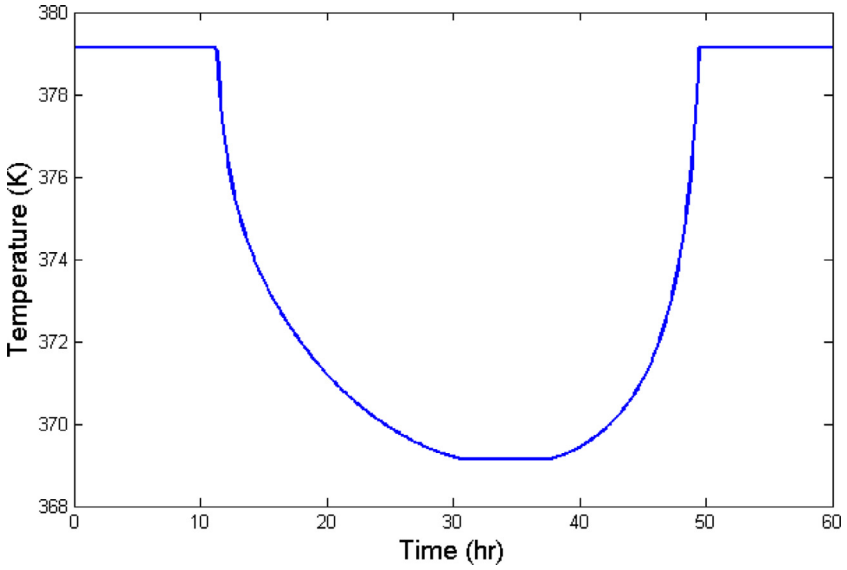

Fig. 10. Optimal temperature profile for the thermal hydrolysis case-study.

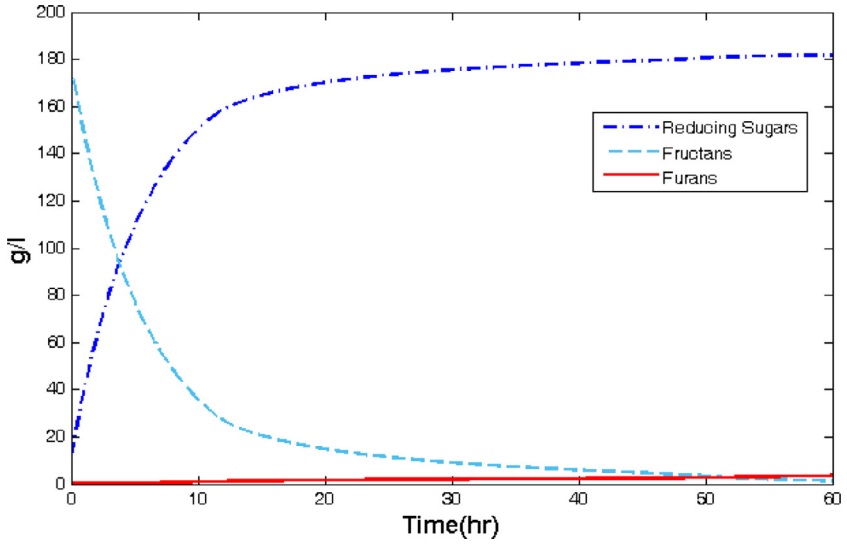

Fig. 11. Optimal profiles for the thermal hydrolysis case-study.

formation approach are significant in the case of an optimization problem.

(vi) For the example of the administration of amiodarone, a continuous optimal profile for the infusion rate was determined. For practical considerations in this particular example, an alternative approach was provided for the case that the administration route of the drug requires discrete doses at given times during the treatment. The optimal results are quite similar to those obtained by Herceg et al. (2017), who studied an analogous administration route for amiodarone, but following a rational approximation approach.

On the other hand, one of the limitations of this work is still the size of the problems that have been solved through the proposed approach. No large-scale problems have been tested yet. On this regard, from the computational point of view, the performance of the gradient method in the fractional-ordinary case is similar from its performance in the ordinary case; its convergence capabilities as well as the computational effort needed are significantly affected when the number of control variables is increased. That is of course a relevant issue on large scale problems. Therefore, alternative techniques should be explored to solve the two-point fractional-ordinary boundary value problem which results from the Euler-Lagrange Optimality conditions used on this paper. In fact, fractional-ordinary optimal control problems could also be approached by direct transcription methods; for such case, however, efficient discretization methods for fractional-ordinary problems in the time domain would be needed. Finally, as another additional guidance for future work, large-scale case-studies involving fractional-ordinary equations are still to be developed; the real-world applications described by Sun et al. (2018) appear as excellent suggestions to complete such task.

Declaration of Competing Interest

The authors declare that they have no known competing financial interests or personal relationships that could have appeared to influence the work reported in this paper.

Acknowledgements

The authors thank the financial support provided by the Mexican National Council for Science and Technology (CONACYT) 257018 and the Mexican National Institute of Technology (TNM) 5725.16-P.

Supplementary materials

Supplementary material associated with this article can be found, in the online version, at doi:10.1016/j.compchemeng.2019.106638.

References

Agrawal, O.P., 2002. Formulation of Euler–Lagrange equations for fractional variational problems. J. Math. Anal. Appl. 272 (1), 368–379. doi:10.1016/S0022-247X(02)00180-4.

Agrawal, O.P., 2004. A general formulation and solution scheme for fractional optimal control problems. Nonlinear Dyn. 38 (1-4), 323–337. doi:10.1007/s11071-004-3764-6.

Agrawal, O.P., 2007. Generalized Euler—Lagrange equations and transversality conditions for FVPs in terms of the Caputo derivative. J. Vib. Control 13 (9-10), 1217–1237. doi:10.1177/1077546307077472.

Agrawal, O.P., 2008. A formulation and numerical scheme for fractional optimal control problems. J. Vib. Control 14 (9-10), 1291–1299. doi:10.3182/20060719-3-PT-4902.00011.

Agrawal, O.P., 2010. Generalized variational problems and Euler–Lagrange equations. Comput. Math. Appl. 59 (5), 1852–1864. doi:10.1016/j.camwa.2009.08.029.

Aguila-Camacho, N., Duarte-Mermoud, M.A., 2017. Combined Fractional Adaptive Control. Int. Feder. Autom. Control PapersOnLine 50 (1), 8586–8591. doi:10.1016/j.ifacol.2017.08.1423.

Almeida, R., 2017. Variational problems involving a Caputo-type fractional derivative. J. Optim. Theory Appl. 174, 276–294. doi:10.1007/s10957-016-0883-4.

Almeida, R., Torres, D.F., 2011. Necessary and sufficient conditions for the fractional calculus of variations with Caputo derivatives. Commun. Nonlinear Sci. Numer. Simul. 16 (3), 1490–1500. doi:10.1016/j.cnsns.2010.07.016.

Andrés-Martínez, O., Flores-Tlacuahuac, A., Kameswaran, S., Biegler, L.T., 2019. An efficient direct/indirect transcription approach for singular optimal control. AIChE J 65 (3), 937–946. doi:10.1002/aic.16487.

Atanackovic, T.M., Janev, M., Pilipovic, S., Zorica, D., 2017. Euler–Lagrange equations for Lagrangians containing complex-order fractional derivatives. J. Optim. Theory Appl. 174, 256–275. doi:10.1007/s10957-016-0873-6.

Baleanu, D., Trujillo, J.I., 2010. A new method of finding the fractional Euler–Lagrange and Hamilton equations within Caputo fractional derivatives. Commun. Nonlinear Sci. Numer. Simul. 15 (5), 1111–1115. doi:10.1016/j.cnsns.2009.05.023.

Copot, D., Chevalier, A., Ionescu, C.M., De Keyser, R., 2013. A two-compartment fractional derivative model for propofol diffusion in anesthesia. In: Control Applications (CCA). 2013 IEEE International Conference, pp. 264–269. doi:10.1109/CCA.2013.6662769.

Copot, D., De Keyser, R., Derom, E., Ionescu, C., 2017a. Structural changes in the COPD lung and related heterogeneity. PLoS One 12 (5), e0177969. doi:10.1371/journal.pone.0177969.

Copot, D., Magin, R.L., De Keyser, R., Ionescu, C., 2017b. Data-driven modelling of drug tissue trapping using anomalous kinetics. Chaos Solit. Fract. 102, 441–446. doi:10.1016/j.chaos.2017.03.031.

Diethelm, K., 2010. The analysis of fractional differential equations. Lecture Notes in Mathematics, 2004. Springer: Berlin, Germany Volume.

Diethelm, K., 2013. A fractional calculus based model for the simulation of an outbreak of dengue fever. Nonlinear Dyn. 71 (4), 613–619. doi:10.1007/s11071-012-0475-2.

Diethelm, K., Ford, N.J., Freed, A.D., 2002. A predictor-corrector approach for the numerical solution of fractional differential equations. Nonlinear Dyn. 29 (1), 3–22. doi:10.1023/A:1016592219341.

Diethelm, K., Ford, N.J., Freed, A.D., 2004. Detailed error analysis for a fractional Adams method. Numer. Algorithms 36 (1), 31–52. doi:10.1023/B:NUMA.0000027736.85078.be.

Diethelm, K., Ford, N.J., Freed, A.D., Luchko, Y., 2005. Algorithms for the fractional calculus: a selection of numerical methods. Comput. Meth. Appl. Mech. Eng. 194 (6), 743–773. doi:10.1016/j.cma.2004.06.006.

Ding, Y., Wang, Z., Ye, H., 2012. Optimal control of a fractional-order HIV-immune system with memory. IEEE Trans. Control Syst. Technol. 20 (3), 763–769. doi:10.1109/TCST.2011.2153203.

Dokoumetzidis, A., Magin, R., Macheras, P., 2010a. A commentary on fractionalization of multi-compartmental models. J. Pharmacokinet. Pharmacodyn. 37 (2), 203–207. doi:10.1007/s10928-010-9153-5.

Dokoumetzidis, A., Magin, R., Macheras, P., 2010b. Fractional kinetics in multi-compartmental systems. J. Pharmacokinet. Pharmacodyn. 37 (5), 507–524. doi:10.1007/s10928-010-9170-4.

Flores-Tlacuahuac, A., Biegler, L.T., 2014. Optimization of fractional order dynamic chemical processing systems. Ind. Eng. Chem. Res. 53 (13), 5110–5512. doi:10.1021/ie401317r.

Garcia-Soto, M.J., Jiménez-Islas, H., Navarrete-Bolaños, J.L., Rico-Martinez, R., Miranda-López, R., Botello-Alvarez, J.E., 2011. Kinetic study of the thermal hydrolysis of Agave salmiana for mezcal production. J. Agric. Food Chem. 59 (13), 7333–7340. doi:10.1021/jf200026y.

Garrapa, R., 2018. Numerical solution of fractional differential equations: a survey and a software tutorial. Mathematics 6, 16. doi:10.1007/10.3390/math6020016.

Guo, T.L., 2013. The necessary conditions of fractional optimal control in the sense of Caputo. J. Optim. Theory Appl. 156 (1), 115–126. doi:10.1007/s10957-012-0233-0.

Hennion, M., Hannert, E., 2013. How to avoid unbounded drug accumulation with fractional Pharmacokinetics. J. Pharmacokinet. Pharmacodyn. 40, 691–700. doi:10.1007/s10928-013-9340-2.

Herceg, D., Ntouskas, S., Sopasakis, P., Dokoumetzidis, A., Macheras, P., Sarimveis, H., Patrinos, P., 2017. Modeling and administration scheduling of fractional-order pharmacokinetic systems. IFAC World Congress-Papers Line 50 (1), 9742–9747. doi:10.1016/j.ifacol.2017.08.2178.

Herzallah, M.A., Baleanu, D., 2009. Fractional-order Euler–Lagrange equations and formulation of Hamiltonian equations. Nonlinear Dyn. 58 (1), 385–391. doi:10.1007/s11071-009-9486-z.

Ionescu, C., Copot, D., De Keyser, R., 2016. Modelling Doxorubicin effect in various cancer therapies by means of fractional calculus. In: Proceedings of the American Control Conference (ACC). IEEE, pp. 1283–1288. doi:10.1109/ACC.2016.7525094.

Ionescu, C., Kelly, J.F., 2017. Fractional calculus for respiratory mechanics: Power law impedance, viscoelasticity, and tissue heterogeneity. Chaos Solit. Fract. 102, 433–440. doi:10.1016/j.chaos.2017.03.054.

Ionescu, C., Lopes, A., Copot, D., Machado, J.A.T., Bates, J.H.T., 2017. The role of fractional calculus in modeling biological phenomena: A review. Commun. Nonlinear Sci. Numer. Simul. 51, 141–159. doi:10.1016/j.cnsns.2017.04.001.

Ionescu, C., Tenreiro Machado, J., De Keyser, R., Decruyenaere, J., Struys, M.M.R.F., 2015. Nonlinear dynamics of the patient's response to drug effect during general anesthesia. Commun. Nonlinear Sci. Numer. Simul. 20, 914–926. doi:10.1016/j.cnsns.2014.05.014.

Ionescu, C.M., Copot, D., De Keyser, R., 2013. Respiratory impedance model with lumped fractional order diffusion compartment. IFAC Proceedings Volumes 46 (1), 260–265. doi:10.3182/20130204-3-FR-4032.00084.

Jahanshahi, S., Torres, D.F.M., 2017. A simple accurate method for solving fractional variational and optimal control problems. J. Optim. Theory Appl. 174, 156–175. doi:10.1007/s10957-016-0884-3.

Jelicic, Z.D., Petrovacki, N., 2009. Optimality conditions and a solution scheme for fractional optimal control problems. Struct. Multidisc. Optim. 38 (6), 571–581. doi:10.1007/s00158-008-0307-7.

Kovács, L., Benyó, B., Bokor, J., Benyó, Z., 2011. Induced L_2-norm minimization of glucose–insulin system for Type I diabetic patients. Comput. Methods Progr. Biomed. 102, 105–118. doi:10.1016/j.cmpb.2010.06.019.

Li, Y., Chen, Y.Q., Podlubny, I., 2009. Mittag–Leffler stability of fractional order nonlinear dynamic systems. Automatica 8 (45), 1965–1969. doi:10.1016/j.automatica.2009.04.003.

Lopes, A.M., Tenreiro-Machado, J.A., Galhano, A.M., 2019. Towards fractional sensors. J. Vib. Control 25 (1), 52–60. doi:10.1177/1077546318769163.

Lubich, C., 1986. Discretized fractional calculus. SIAM J. Math. Anal. 17 (3), 704–719. doi:10.1137/0517050.

Magin, R., 2004. Fractional calculus in bioengineering. Begell House, Inc. Publishers, CT, USA.

Magin, R.L., 2010. Fractional calculus models of complex dynamics in biological tissues. Comput. Math. Appl. 59, 1586–1593. doi:10.1016/j.camwa.2009.08.039.

Mendes, E.M.A.M., Salgado, G.H.O., Aguirre, L.A., 2019. Numerical solution of Caputo fractional differential equations with infinity memory effect at initial condition. Commun. Nonlinear Sci. Numer. Simul. 69, 237–247. doi:10.1016/j.cnsns.2018.09.022.

Moghaddam, B.P., Dabiri, A., Lopes, A.M., Tenreiro Machado, J.A., 2019. Numerical solution of mixed-type fractional functional differential equations using modified Lucas polynomials. Comput. Appl. Math. 38, 46. doi:10.1007/s40314-019-0813-9.

Nuno, R., Bastos, O., 2018. Calculus of variations involving Caputo–Fabrizio fractional differentiation. Statist. Optim. Inf. Comput. 6, 12–21. doi:10.19139/soic.v6i1.466.

Pakdaman, M., Ahmadian, A., Effati, S., Salahshour, S., Baleanu, D., 2017. Solving differential equations of fractional order using an optimization technique based on training artificial neural network. Appl. Math. Comput. 293, 81–95. doi:10.1016/j.amc.2016.07.021.

Pereira, L.M., 2010. Fractal pharmacokinetics. Comput. Math.Methods Med. 11 (2), 161–184. doi:10.1080/17486700903029280.

Petráš, I., Magin, R.L., 2011. Simulation of drug uptake in a two compartmental fractional model for a biological system. Commun. Nonlinear Sci. Numer. Simul. 16, 4588–4595. doi:10.1016/j.cnsns.2011.02.012.

Popović, J.K., Atanacković, M.T., Pilipović, A.S., Rapaić, M.R., Pilipović, S., Atanacković, T.M., 2010. A new approach to the compartmental analysis in pharmacokinetics: fractional time evolution of diclofenac. J. Pharmacokinet. Pharmacodyn. 37 (2), 119–134. doi:10.1007/s10928-009-9147-3.

Rabiei, K., Parand, K., 2019. Collocation method to solve inequality-constrained optimal control problems of arbitrary order. Eng. Comput. 1–11. doi:10.1007/s00366-018-0688-1.

Rakhshan, S.A., Effati, S., Kamyad, A.V., 2018. Solving a class of fractional optimal control problems by the Hamilton–Jacobi–Bellman equation. J. Vib. Control 24 (9), 1741–1756. doi:10.1177/1077546316668467.

Sales Teodoro, G., Tenreiro Machado, J.A., Capelas de Oliveira, E., 2019. A review of

definitions of fractional derivatives and other operators. J. Comput. Phys. 388, 195–208. doi:10.1016/j.jcp.2019.03.008.
Sápi, J., Drexler, D.A., Kovács, L., 2017. Potential benefits of discrete-time controller-based treatments over protocol-based cancer therapies. Acta Polytechnica Hungarica 14 (1), 11–23. doi:10.12700/APH.14.1.2017.1.2.
Sarafnia, N., Malekzadeh, M., Askari, J., 2018. Fractional order PDD control of spacecraft rendezvous. Adv. Space Res. 62, 1813–1825. doi:10.1016/j.asr.2018.06.040.
Sopasakis, P., Sarimveis, H., 2017. Stabilising model predictive control for discrete-time fractional-order systems. Automatica 75, 24–31. doi:10.1016/j.automatica.2016.09.014.
Srinivasan, B., Palanki, S., Bonvin, D., 2003. Dynamic optimization of batch processes: I. Characterization of the nominal solution. Comput. Chem. Eng. 27 (1), 1–26. doi:10.1016/S0098-1354(02)00116-3.
Stengel, R.F., 1994. Optimal Control and Estimation. Dover Publications Inc., New York, USA, p. 186.
Sun, H.G., Zhang, Y., Baleanu, D., Chen, W., Chen, Y.Q., 2018. A new collection of real world applications of fractional calculus in science and engineering. Commun. Nonlinear Sci. Numer. Simul. 64, 213–231.
Tenreiro-Machado, J.A., Silva, M.F., Barbosa, R.S., Jesus, I.S., Reis, C.M., Marcos, M.G., Galhano, A.F., 2010. Some applications of fractional calculus in engineering. Math. Probl. Eng. 2010, 1–34. doi:10.1155/2010/639801.
Toledo-Hernandez, R., Rico-Ramirez, V., Iglesias-Silva, G.A., Diwekar, U.M., 2014a. A fractional calculus approach to the dynamic optimization of biological reactive systems. Part I: fractional models for biological reactions. Chem. Eng. Sci. 117, 217–228. doi:10.1016/j.ces.2014.06.034.
Toledo-Hernandez, R., Rico-Ramirez, V., Rico-Martinez, R., Hernandez-Castro, S., Diwekar, U.M., 2014b. A fractional calculus approach to the dynamic optimization of biological reactive systems. Part II: Numerical solution of fractional optimal control problems. Chem. Eng. Sci. 117, 239–247. doi:10.1016/j.ces.2014.06.033.
Tricaud, C., Chen, Y., 2010. An approximate method for numerically solving fractional order optimal control problems of general form. Comput. Math. Appl. 59 (5), 1644–1655. doi:10.1016/j.ces.2014.06.033.
Wei, Y., Du, D., Cheng, S., Wang, Y., 2017. Fractional order systems time-optimal control and its application. Optim. Theory Appl. 174, 122–138. doi:10.1007/s10957-015-0851-4.
West B.J., Bologna M., Grigolini P. (2003) Fractional Rheology. In: Physics of Fractal Operators. Institute for Nonlinear Science. Springer, New York, NY.
Yang, F., Zhu, K., 2011. On the definition of fractional derivatives in rheology. Theor. Appl. Mech. Lett. 1 (1), 012007. doi:10.1063/2.1101207.
Zecova, M., Terpak, J., 2015. Heat conduction modeling by using fractional-order derivatives. Appl. Math. Comput. 257, 365–373. doi:10.1016/j.amc.2014.12.136.